POLITECNICO DI MILANO

DIPARTIMENTO DI INGEGNERIA CIVILE E AMBIENTALE

Corso di Laurea Magistrale in Ingegneria per l'Ambiente e il Territorio

Tesi di laurea magistrale

Modelling of calcite and dolomite dissolution in the Buffered Accelerated Weathering of Limestone technology for CO_2 storage

Candidato:
Selene Varliero
Matricola 918881

Relatore:
Prof. Stefano Caserini

Correlatore:
Prof. Guido Raos

Anno Accademico 2020/2021

Contents

List of Figures

List of Tables

Chapter 1

Introduction

Anthropogenic CO_2 emissions have increased the global mean surface temperature of 0.8-1.2 °C from the pre-industrial era (Masson-Delmotte et al. 2018). The "Paris Agreement", signed in 2015 at United Nations Climate Change Conference COP 21 by 196 parties, aims to limit global warming well below 2°C above pre-industrial levels and attempt not to exceed 1.5°C of temperature increase: climate change's environmental and social impact will be amplified if this commitment is not respected (Portner et al. 2019).

Different strategies can be actualized to limit the global worming at 1.5°C above the pre-industrial level (Figure 1.1). Reduction of CO_2 emissions and usage of Carbon Dioxide Removal (CDR) strategies are both essential: CDR should remove from 100 to 1000 $GtCO_2$ in the current century to limit the temperature increase to 1.5°C (Rogelj et al. 2018).

The IPCC (International Panel on Climate Change) classified the different CDR technologies into six groups (Coninck et al. 2018):

- Bioenergy with carbon capture and storage (BECCS);
- Afforestation and reforestation (AR);
- Soil carbon sequestration and biochar;
- Enhanced weathering (EW) and ocean alkalization;
- Direct air carbon dioxide capture and storage (DACCS);
- Ocean fertilization.

CDR measures represent a set of options, each of which will contributes in different proportions to the reduction of CO_2 (Rogelj et al. 2018). Indeed there is not a specific CDR technology that is still available to remove all the

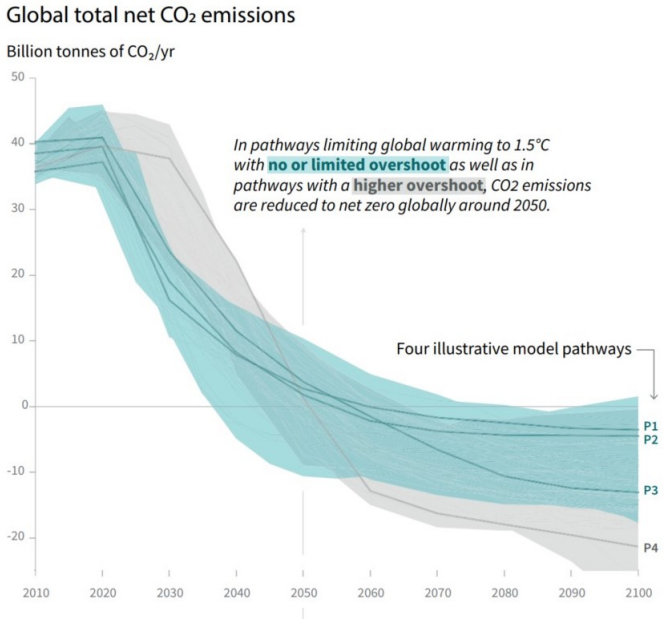

Figure 1.1: Representation of different global CO_2annual emission scenarios that will limit the global warming temperature increase to 1.5°C (Masson-Delmotte et al. 2018).

necessary CO_2 to prevent the global temperature increase of 2°C, and each technology has a distinct impact on the environment and society; therefore, the choice may change in different contexts (Rogelj et al. 2018).

Among the different CDR techniques, a crucial point is represented by the storage of carbon dioxide. Indeed, BECCS is considered as one of the most post potential technology to implement negative emissions (Bui et al. 2018; Rogelj et al. 2018), and its operating principle is divided into two phases: first energy is produced by biomass, then CO_2 emitted by biomass exploitation is captured and stored. Even if the carbon dioxide storage can be done with different techniques, BECCS is usually associated with geological storage.

Figure 1.2 shows the stage of development of different technologies involved in the capture and storage of CO_2. The CO_2 storage technologies currently used are geological storage combined with enhanced oil recovery and storage in deep saline aquifer (Bui et al. 2018). The first technology has a higher capacity: potentially, it could store all the carbon dioxide needed to limit global warming to 1.5°C (Bui et al. 2018) but actually the operative installation can contain about 40 Mt of carbon dioxide year (Page et al. 2020), a value that is not sufficient to store all the carbon dioxide required accord-

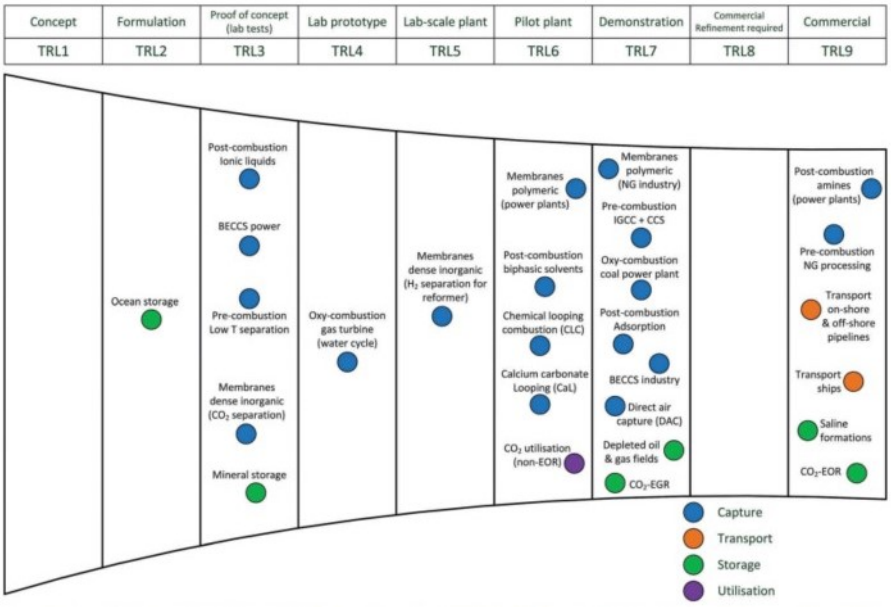

Figure 1.2: Diagram that shows the degree of development of different technologies for the capture, transport, storage and utilization of CO_2 (Bui et al. 2018)

.

ing to IPCC. Moreover, the existing CCS structure are mainly encouraged by the profit of enhanced oil recovery (Page et al. 2020) that reduces the net CO_2 storage.

Enhanced weathering processes consist of speeding up the natural geochemical reactions that convert atmospheric CO_2 into carbonate minerals or bicarbonate ions.

An exemplifying weathering process is the silicate weathering, which is recognized as one of the negative feedback that, on a geological scale ($>$ 100,000 years), contributes to Earth's temperature regulation (Archer 2005; Walker, Hays, and Kasting 1981). Different applications take inspiration from this natural process and use powdered silicate as a soil additive. In this way the mineral (e.g. olivine $(Mg, Fe)_2SiO_4$) reacts with CO_2 in the atmosphere, producing bicarbonate ions (HCO_3^-), which add alkalinity to acid soils and adsorb CO_2 (Renforth, Strandmann, and Henderson 2015; Schuiling and Krijgsman 2006).

While enhanced silicate weathering adsorbs carbon dioxide directly from the atmosphere, other technologies combine enhanced weathering with the necessity to store CO_2 produced in industrial plants. Rau and Caldeira have

first proposed a technology defined as Accelerated Weathering of Limestone (AWL). Its principle is to store CO_2 in ocean as bicarbonate ions, by creating a solution of carbon dioxide, limestone and seawater, that can be discharged in the surface layer of ocean (Rau and Caldeira 1999).

Other studies have analyzed extensively AWL, for examples, how to set the different technology parameters and how to structure the industrial plant. But the main disadvantage is that part of the CO_2 is again released by the ocean, due the low depth of discharge and incomplete conversion of carbon dioxide in bicarbonate ions (W. C. Chou et al. 2015; Kirchner, Lettmann, et al. 2020; Rau 2011).

The technology studied in this thesis is named Buffered Accelerated Weathering of Limestone (BAWL), a CO_2 storage technology in a stage of formulation (TRL2). BAWL proposes an alternative technology to AWL to avoids the CO_2 degassing. Its features are presented in chapter 2.

Chapter 3 introduces the theoretical chemical reactions on which the AWL and BAWL processes are based on.

AWL and BAWL presupposes the use of limestone, a sedimentary carbonate rock composed primarily of calcite ($CaCO_3$), but it can theoretically work with other kinds of carbonate minerals (e.g. dolomite $CaMg(CO_3)_2$, magnesite $MgCO_3$). One of the aims of this thesis is to assess if dolomite could substitute calcite in BAWL functioning, on this purpose the chapter 4 focus on dolomite and calcite dissolution in water, and its modeling on the software PHREEQC, which is utilized to simulate the BAWL functioning.

In chapter 5, BAWL working parameters are presented and analyzed within PHREEQC, to identify different feasible operating points both for calcite and dolomite utilization. In chapter 6 these points are examined deeper, also by a preliminary costs analysis.

Chapter 2

Buffered Accelerated Weathering of Limestone

2.1 Accelerated Weathering of Limestone and Buffered Accelerated Weathering of Limestone

BAWL is based on Accelerated Weathering of Limestone process proposed by Rau et Caldeira that introduced the system represented in Figure 2.1: a reactor in which seawater can flow through a medium made of carbonate minerals (as calcite) and contemporary a CO_2-rich gas stream is injected counter-current in the same reactor (Rau and Caldeira 1999). The resulting solution is then re-injected in ocean, with the result of storing CO_2 as bicarbonate ions and add alkalinity to seawater.

The main disadvantages of this setup are:

- The high AWL consumption of seawater: a minimum 7000 t of H_2O for each tonne of CO_2 stored.
- The fact that 15% of CO_2 injected in solution is released again in atmosphere, so AWL does not guarantee a long-lasting storage.

The CO_2 degassing happens because part of carbon dioxide contained in discharged solution does not react with limestone, but remains dissolved as hydrated CO_2. Since the discharge point is in the surface layers of ocean, the solution balances with atmosphere, and CO_2 is released from the ocean.

Different studies are performed on AWL, analyzing distinct reactor set-up (W. C. Chou et al. 2015) and discharge scenarios (Kirchner, Lettmann, et al. 2020). An AWL pilot plant is installed in a coal power-plant in Germany,

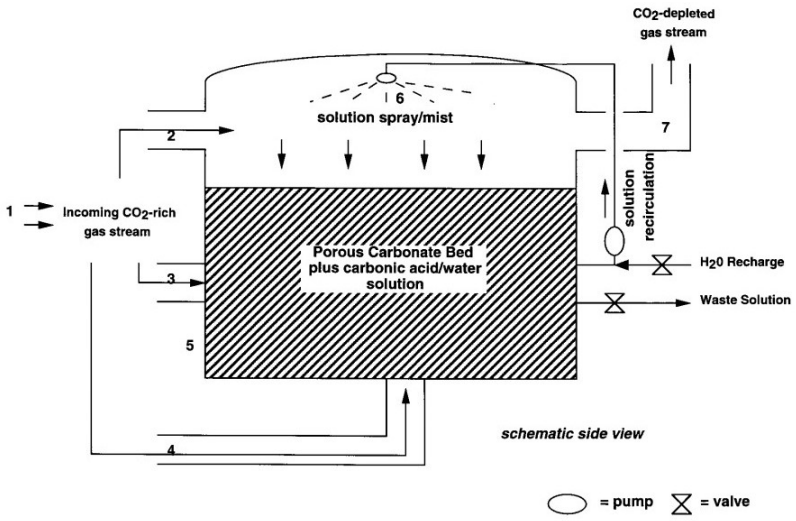

Figure 2.1: AWL configuration for CO_2 sequestration as bicarbonate, figure by Rau and Caldeira, 1999.

on North Sea (Kirchner, Berry, et al. 2020). Positive results from the plant indicate that negative impact on marine biota are not observed, but about only the 50% of CO_2 stored is not released in atmosphere after the seawater discharge.

Buffered Accelerated Weathering of Limestone proposes different modifications in AWL process (Caserini et al. 2021; Righi 2020).

- The reaction among limestone, CO_2 and seawater does not occur on land in a dedicated reactor, but calcite is powdered and injected directly in the pipeline that channels the solution of seawater and CO_2 in ocean.
- The pipeline discharge is not in the surface layers of ocean but deeper, where pressure limits carbon dioxide degassing and facilitate the complete reaction of hydrated CO_2. Moreover, a higher pressure speeds up and enhances the chemical reactions, lowering the water requirement and the amount of unreacted CO_2.
- $Ca(OH)_2$ is used as buffer for the unreacted CO_2, this process ensures a final pH comparable with natural seawater level ($\cong 8$).

As AWL, the BAWL is a technology that stores CO_2 in seawater by adding alkalinity to the ocean. But differently from AWL, it will require a lower amount of water on the same quantity of carbon dioxide and the storage will be long-lasting thanks to the avoided degassing of CO_2.

The process is divided in different steps:

- CO_2 dissolution in seawater.
- Injection of mineral powder in the solution.
- Solution is channeled into a pipeline, which end well below ocean surface. The complete dissolution of carbonate mineral and its reaction with carbon dioxide occur in this pipeline.
- Calcium hydroxide, through a dedicated pipeline, is added at the solution in the final section of the pipeline and reacts with the remaining carbon dioxide.
- The solution is released in the ocean, with mineral carbonate, carbon dioxide and calcium hydroxide already reacted.
- The plume is diluted in the ocean.

2.2 BAWL component

In section 6.1.1, the different features of the proposed process are described in greater detail, but the main installations of BAWL are here described. It is important to remind that there is not an existing plant that implemented BAWL, and different aspect of of the technology requirement should be still defined.

Milling processes It is necessary to grind calcite, used in the dissolution reactor with CO_2 and for production of calcium hydroxide.

Calcination $Ca(OH)_2$ is produced directly at the plant by a process that intrinsically releases CO_2 (see chapter 3); this emission will be directly captured and stored with BAWL.

CO_2, limestone and seawater mixer Commercially, different types of reactors are available to dissolve a gas into a liquid solution. For our purpose, the configurations taken into exam are a bubble-type adsorption column or a packed bed adsorption column. Both are designed as a vertical reactor with closed headspace: this expedient prevents the release of seawater aerosol and carbon dioxide in the environment and allows the re-circulation of CO_2.

The gaseous flux containing CO_2 can be composed of pure CO_2, to enhance its transfer to water, but it could be also a flue gas already purified

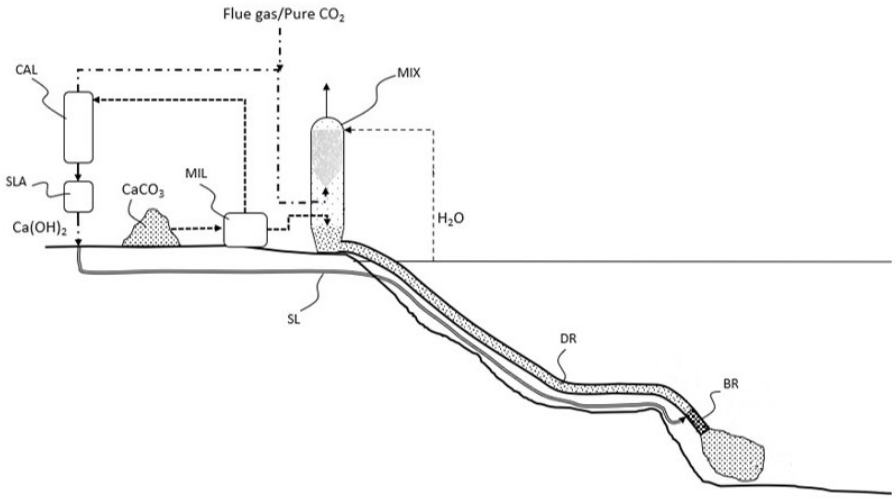

Figure 2.2: General scheme of BAWL plant (Cappello et al. 2021)

from dangerous compounds. It is not necessary to bring CO_2 to the supercritical state as in other technologies, like geological storage.

Dissolution Reactor - Carbonate minerals pipeline The pipeline is the dissolution reactor (DR) in which carbonate minerals will dissolve and react with carbon dioxide, so its length and depth are bound to the kinetics requisites of time and pressure (see chapter 5).

The pipeline can be realized in commercialized HDPE, and installed on the seabed.

Complications will occur if slurry sediments in the pipeline, but this can be overcome by guaranteeing a minimum flow velocity of 1.2 ms^{-1} that will prevent sedimentation of particles of 50 μm or smaller.

Slacked lime pipeline - Calcium hydroxide pipeline This secondary pipeline brings the calcium hydroxide (slacked lime), solubilized in seawater, close to the end of the previous pipeline.

Slacked lime (SL) pipeline has similar characteristics as DR, but the flow rate that transports is lower so the pipeline diameter is smaller.

Buffering reactor At the end of the dissolution reactor, an extension section is present to allow the reaction between $Ca(OH)_2$ and CO_2, this pipeline segment is the buffering reactor (BR). The main concern about this process phase is the possible precipitation of calcium carbonate due to the high pH,

so the reactor should be short as possible but enough long to guarantee a complete flow mixing, about 20-30 meters in length.

Chapter 3

Carbonate species interaction in water

Natural water contains inorganic carbonate species, mainly CO_2, HCO_3^- and CO_3^{2-}. Which are in a equilibrium that can be expressed by reaction 3.1:

$$CO_2 \rightleftharpoons H^+ + HCO_3^- \rightleftharpoons 2\,H^+ + CO_3^{2-} \tag{3.1}$$

The equilibrium is regulated mainly by the pH of the solution, as seen in Figure 3.1. At the natural pH of seawater (≈ 8) the main form present of inorganic carbon is bicarbonate ions.

In the natural geological cycle, the ocean is in equilibrium with the atmosphere and absorbs CO_2 accordingly to Henry's law. But since the industrial revolution, CO_2 levels in the atmosphere are increased and the ocean starts absorbing more CO_2, acting like a sink that has adsorbed the 20-30% of total anthropogenic CO_2 emitted since 1980 (Portner et al. 2019). This phenomenon changes the carbonate chemistry of the ocean, and an ocean

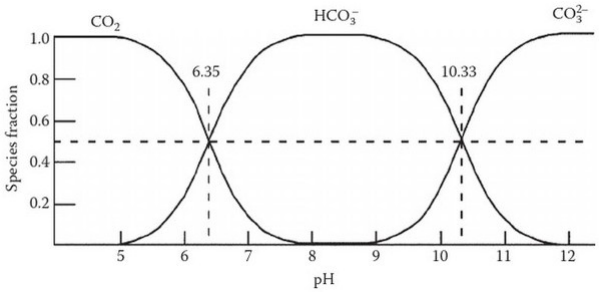

Figure 3.1: Distribution of the main carbonate species in freshwater, depending on pH (Weiner 2012).

acidification process is started, characterized by a speed unprecedented for at least 65 million years (Hoegh-Guldberg et al. 2018).

The reactions that take place in a water-based solution after the addition of CO_2 are represented in the equations system 3.2: once in aqueous form, the carbon dioxide react with water forming carbonic acid H_2CO_3, which dissociate decreasing the pH of the solution.

$$CO_2\,(g) \rightleftharpoons CO_2\,(aq) \tag{3.2a}$$

$$CO_2\,(aq) + H_2O \rightleftharpoons H_2CO_3 \tag{3.2b}$$

$$H_2CO_3 \rightleftharpoons H^+ + HCO_3{}^- \tag{3.2c}$$

$$HCO_3{}^- \rightleftharpoons H^+ + CO_3{}^{2-} \tag{3.2d}$$

Regarding reaction 3.2b, usually at the equilibrium, the concentration of CO_2 is 600 times higher than the ones of carbonic acid, so the sum of CO_2 and H_2CO_3 in the solution is indicated as $H_2CO_3{}^*$ (C Anthony J Appelo and Postma 2004). It is essential to highlight that the reactions have all different time scale, in particular CO_2 dissolves in water (reaction 3.2a) almost instantly compared to the other reaction (Mitchell et al. 2010). This is why in the following sections, the time required for carbon dioxide dissolution is not considered explicitly.

If the injection of CO_2 is combined with the dissolution of a carbonate mineral as calcite ($CaCO_3$), the reaction that takes place is described by equation 3.3. In this case, carbonic acid does not release hydrogen ions but only calcium and bicarbonate ions, increasing the buffer capacity of the solution.

$$CaCO_3 + H_2CO_3 \rightleftharpoons Ca^{2+} + 2\,HCO_3{}^- \tag{3.3}$$

The net reaction of CO_2 and calcite dissolution in water is expressed in equation 3.4:

$$CO_2 + CaCO_3 + H_2O \rightleftharpoons Ca^{2+} + 2\,HCO_3{}^- \tag{3.4}$$

Reaction 3.4 is the one implemented in AWL application: it is important to consume carbon dioxide and carbonate mineral to store CO_2 and add alkalinity to seawater. This purpose can also be achieved with different minerals other than calcite; reactions 3.5 and 3.6 show respectively how dolomite and magnesite will react with CO_2 and water. Moreover, other crystal forms of calcite (e.g. aragonite) can be used; in this case, the reaction 3.4 is still valid.

$$2\,CO_2 + CaMg(CO_3)_2 + 2\,H_2O \rightleftharpoons Ca^{2+} + Mg^{2+} + 4\,HCO_3{}^- \tag{3.5}$$

$$CO_2 + MgCO_3 + H_2O \rightleftharpoons Mg^{2+} + 2\,HCO_3^- \tag{3.6}$$

For BAWL application, calcite is the most studied mineral because it is abundant in nature and characterized by fast dissolution kinetics compared to other carbonate minerals (L. Chou, Garrels, and Wollast 1989). In this work, dolomite is examined to assess if it could substitute calcite.

Dolomite can be found in two different form: sedimentary and hydrothermal. These two minerals differs from the process formation that causes different crystal lattice, namely the sedimentary dolomite has a disordered lattice than the hydrothermal. Since a mineral of ordered lattice needs an higher activation energy to dissolve, we expect that the reaction of sedimentary dolomite will be faster (Palandri and Kharaka 2004).

3.1 Calcium hydroxide and carbon dioxide reaction

As explained in chapter 5, BAWL operates with an excess of carbon dioxide to ensure the complete dissolution of carbonate minerals and that the remaining CO_2 will be neutralized with calcium hydroxide.

Calcium hydroxide is usually produced by calcination, a process described by equation 3.7. Starting from a carbonate mineral as limestone and giving energy to the system, the calcium oxide is produced, which, with the addition of water, gives the hydroxide:

$$CaCO_{3(s)} \longrightarrow CaO_{(s)} + CO_{2(g)} \tag{3.7}$$

$$CaO_{(s)} + H_2O_{(aq)} \longrightarrow Ca(OH)_{2(s)} \tag{3.8}$$

As it is show in reaction 3.7, to produce one mole of calcium hydroxide one mole of carbon dioxide will be produced. Moreover, equation 3.7 is highly endothermic (standard enthalpy of reaction $\Delta H_{0r} = 178.3 kJmol^{-1}$) so it will require an high energy to take place. These energy can be supplied by an electric process not originated by fossil fuel, in this way the CO_2 emitted by calcination is limited to that produced in reaction 3.7. Equation 3.8 is exothermic (standard enthalpy of reaction $\Delta H_{0r} = -65.17 kJmol^{-1}$), and some of the heat produced may be recovered and used for reaction 3.7.

In water, calcium hydroxide reacts with carbon dioxide as reported below:

$$2\,CO_2 + Ca(OH)_2 \longrightarrow Ca(HCO_3)_2 \tag{3.9}$$

Chapter 4

Implementation of carbonate mineral dissolution in PHREEQC

PHREEQC is a software developed by the U. S. Geological Survey (USGS); it is expressly devoted to geochemistry modelling and can be applied to different kinds of situations as transport in aquifers, gas-water-solid interaction, water speciation. It can be applied for freshwater, brine or seawater, depending on the database used. BEWL works with seawater, so the database used is that of default: *phreeqc*, which is suitable for fresh and salty water with an ionic strength under 1 (the ionic strength of seawater is around 0.7) (C. Appelo 2015).

Diffusion phenomena may be treated with a one-dimensional model, assuming concentration gradients along one direction. However, as software implements chemical reaction by dividing the kinetics into time steps treated as a series of batch reactors integrated with Runge-Kutta method, we can assume that all the chemicals are well mixed and the aqueous phases are balanced. This is feasible because in the BAWL pipeline, the turbulent condition is ensured. The time step is chosen of 4 seconds, which gives a good trend of mineral dissolution and allows stabilization of the main species in seawater (Mitchell et al. 2010). The chemical composition of the system is assumed to be controlled by a single reaction, the slowest one, which in BAWL application is the dissolution of minerals. The other chemical components are assumed to be always in equilibrium with the reactants and products of the rate-determining reaction. At the end of each step, PHREEQC return solution speciation and how much the reactant is yet to dissolve. Moreover, throughout the reaction is possible to vary the environmental conditions as temperature and pressure.

Generally, the dissolution of minerals can be described with different models elaborated for distinct purposes. In section 4.1 are reported the main

kinetics models present in the literature.

Other geochemical software are available, e.g. CO2SYS, WATEQ4F, GAMSPATH. Each of them has its specialization; for example, CO2SYS and WATEQ4F do not implement kinetics trend, but only solution speciation (Perkins et al. 1997).

The default database calculates speciation and other characteristics of seawater correctly, but it does not account for some of its specific features.

PHREEQC calculates saturation index as a function of pressure, temperature, and ion activities. However, in seawater, the saturation state of calcite changes not linearly with depth, and the enhancement of rates due to pressure is relevant above 700 dbar (69 atm). However, this effect is weaker at higher depth (Dong et al. 2018). Indeed, as reported in section 4.1, minerals dissolution is bound to saturation index or saturation state (e.g. 4.12 and 4.14).

Another factor omitted by the software is the presence of dissolved organic carbon (DOC) in solution, which seems to be an inhibitor for calcite dissolution in natural seawater (Naviaux et al. 2019).

4.1 Mineral dissolution in PHREEQC

In literature, mineral dissolution is analyzed by different studies. This section reports the main works examined to describe dolomite and calcite dissolution within PHREEQC.

4.1.1 Busenberg and Plummer, 1982

Dolomite and calcite dissolution can be described by the following overall reactions:

$$\mathrm{CaMg(CO_3)_2} \longrightarrow \mathrm{Ca^{2+} + Mg^{2+} + 2\,CO_3{}^{2-}} \tag{4.1}$$

$$\mathrm{CaCO_3} \longrightarrow \mathrm{Mg^{2+} + CO_3{}^{2-}} \tag{4.2}$$

Focusing on dolomite, equation 4.1 can be rewritten highlighting the dependence of dissolution rate on other chemical compounds present in the solutions, namely: H^+, $H_2CO_3{}^*$ and H_2O (Busenberg and N. Plummer 1982). $H_2CO_3{}^*$ represents the sum of CO_2 and H_2CO_3 in the solution (see chapter 3).

The reaction dependence on three different compound, determines distinct dissolution mechanisms that become dominant in acid, neutral or basic pH ranges.

$$\mathrm{CaMg(CO_3)_2 + 2\,H^+ \longrightarrow Ca^{2+} + Mg^{2+} + 2\,HCO_3^-} \tag{4.3}$$

$$\mathrm{CaMg(CO_3)_2 + 2\,H_2CO_3^* \longrightarrow Ca^{2+} + Mg^{2+} + 4\,HCO_3^-} \tag{4.4}$$

$$\mathrm{CaMg(CO_3)_2 + H_2O \longrightarrow Ca^{2+} + Mg^{2+} + 2\,HCO_3^- + 2\,OH^-} \tag{4.5}$$

The forward (or dissolution) rate can be described as a function of H^+, $H_2CO_3^*$ and H_2O, which are the main factors that promote the dissolution:

$$R_f = k_1 a_{H^+}^n + k_2 a_{H_2CO_3^*}^n + k_3 a_{H_2O}^n \tag{4.6}$$

Where:

- R_f: dolomite forward rate ($\mathrm{mmol\,cm^{-2}\,s^{-1}}$).
- k_1, k_2 and k_3: temperature-dependent rate constants that correspond to semi-empirical parameters ($\mathrm{mmol\,cm^{-2}\,s^{-1}}$).
- $a_{H^+}, a_{H_2CO_3^*}, a_{H_2O}$: activities of different ions.
- n: dimensionless coefficient, it expresses the reaction order respect to ions activities.

Dolomite dissolution does not depend linearly from ions activity (equation 4.6). The coefficient n is usually set at 0.5 at 25°C (the work of Chou et al., 1989 set it at 0.75 for temperature of 60°C).

The backward (or precipitation) rate is due to the following reaction:

$$\mathrm{Ca^{2+} + Mg^{2+} + 2\,HCO_3^- + 2\,OH^- \longrightarrow CaMg(CO_3)_2 + H_2O} \tag{4.7}$$

Backward rate can be described with the following equation (Busenberg and N. Plummer 1982):

$$R_b = k_4 a_{HCO_3^-} \tag{4.8}$$

Where:

- R_b: dolomite backward rate ($\mathrm{mmol\,cm^{-2}\,s^{-1}}$).
- k_4: temperature-dependent rate constant that corresponds to semi-empirical parameters ($\mathrm{mmol\,cm^{-2}\,s^{-1}}$).
- $a_{HCO_3^-}$: activities of bicarbonate ions.

The overall dissolution rate of dolomite (and in general of metal carbonate) is often described in literature by polynomial equations that sums the mechanisms of dissolution and precipitation of mineral (Busenberg and N. Plummer 1982; L. Chou, Garrels, and Wollast 1989; L. Plummer, Wigley, and D. Parkhurst 1978).

Equations 4.9 and 4.10 express the calcite and dolomite reaction rates formulated by Busenberg and Plummer (Busenberg and N. Plummer 1982; L. Plummer, Wigley, and D. Parkhurst 1978):

$$R_{Dolomite} = k_1 a_{H^+}^n + k_2 a_{H_2CO_3^*}^n + k_3 a_{H_2O}^n - k_4 a_{HCO_3^-} \tag{4.9}$$

$$R_{Calcite} = k_1 a_{H^+} + k_2 a_{H_2CO_3^*} + k_3 a_{H_2O} - k_4 a_{Ca^{2+}} a_{HCO_3^-} \tag{4.10}$$

Starting from this equation, different kind of kinetics were developed to express the dependence of reaction to parameters as pH and CO_2.

4.1.2 Pokrovsky et al, 2009

Studies as the one of Pokrovsky (Pokrovsky, Golubev, Schott, and Castillo 2009) analyze the dissolution of calcite, dolomite and magnesite in a solution at different temperature, pH and CO_2 concentration. The result is a polynomial equation like:

$$R = A + B \cdot pCO_2 + C \cdot (pCO_2)^2 \tag{4.11}$$

Where:

- R: mineral dissolution rate ($(\mathrm{mol\,cm^{-2}\,s^{-1}})$).
- A, B, C: empirical parameters, calculated for different pH and temperature.
- $p\,CO_2$: carbon dioxide partial pressure (atm).

These types of kinetics are formulated for specific applications, as the CO_2 sequestration in sedimentary basins (Pokrovsky, Golubev, Schott, and Castillo 2009), so are not suitable for BAWL technology.

4.1.3 Appelo et al, 1998

A correct kinetic for the implementation in PHREEQC is the one implemented by (C. Appelo, Verweij, and Schäfer 1998), for calcite dissolution, which is the default calcite rate present in the program (David L Parkhurst,

C. Appelo, et al. 1999). This approach is based on the rate 4.10 but introduces some simplifications: the system should be composed of pure water, calcite, and CO_2, and the aqueous solution should be in contact with a gaseous phase of CO_2 at constant pressure (David L Parkhurst, C. Appelo, et al. 1999).

The result is a rate that includes only the forward rate, while the backward rate is not directly expressed because precipitation mechanism is represented by the saturation index (SI, see equation 5.1), a parameters that indicate the proximity of equilibrium:

$$R = R_f(1 - 10^{\frac{2}{3}SI}) \tag{4.12}$$

The forward rate R_f is the one implemented by Plummer et al (L. Plummer, Wigley, and D. Parkhurst 1978):

$$R_f = k_1 a_{H^+} + k_2 a_{H_2CO_3^*} + k_3 a_{H_2O} \tag{4.13}$$

PHREEQC indicates activity of H_2CO_3* with that of CO_2, because the carbonic acid concentration is usually negligible compared to the carbon dioxide presence (C. Appelo, Beekman, and Oosterbaan 1984; David L Parkhurst, C. Appelo, et al. 1999).

However, equation 4.12 is not implemented for dolomite and in BAWL application CO_2 is not a phase in equilibrium with the solution.

4.1.4 Palandri and Kharaka, 2004

A interesting work is that of Palandri and Kharaka, that describes a general kinetic scheme that is applicable to the dissolution of different minerals in water, and then lists the rate parameters of over 70 minerals (Palandri and Kharaka 2004).

Kinetic implemented is based on the sum of three equations that describe the kinetic in different pH regions: acid, neutral and basic.

$$\begin{aligned}\frac{dn}{dt} = -[&k_{acid} e^{-\frac{E_{acid}}{R}(\frac{1}{T} - \frac{1}{298.15K})} a_{H^+}^{n_1} (1 - \Omega^{p_1})^{q_1} \\ &+ k_{neutral} e^{-\frac{E_{neutral}}{R}(\frac{1}{T} - \frac{1}{298.15K})} (1 - \Omega^{p_2})^{q_2} \\ &+ k_{base} e^{-\frac{E_{base}}{R}(\frac{1}{T} - \frac{1}{298.15K})} a_{H^+}^{n_1} (1 - \Omega^{p_3})^{q_3}]\end{aligned} \tag{4.14}$$

Where:

- $\frac{dn}{dt}$: mineral dissolution rate ($\mathrm{mol\,m^{-2}\,s^{-1}}$).
- k_{acid}, $k_{neutral}$, k_{base}: rate constants at 25°C ($\mathrm{mol\,m^{-2}\,s^{-1}}$).

- E_{acid}, $E_{neutral}$, E_{base}: Arrhenius activation energy E, expressed as ($kJ\,mol^{-2}$).
- R: universal gas constant ($J\,K^{-1}\,mol^{-1}$).
- T: temperature of solution (K).
- Ω: saturation state.
- a_{H^+}: hydrogen ions activity.
- n: reaction order respect to hydrogen ion activity.
- p, q: chemical affinity parameters, equal to 1 for dolomite and calcite.

The rate is directly bound to empirical parameters (k), chemical parameters (E) and operational parameters (T, Ω, a_{H^+}). In this work the precipitation rate is taken into account with the term $(1 - \Omega)$: it implies that the dissolution slows down appreciating the saturation as in the equation 4.12.

The parameters listed by Palandri and Kharaka are reported in Table 4.1. The p_i and q_i coefficients are equal to one for all the carbonate minerals.

Table 4.1: Parameters for calcite and dolomite kinetics, reported from (Palandri and Kharaka 2004)

	Acid Region			Neutral Region		Basic Region		
	Log k	E	n	Log k	E	Log k	E	n
Calcite	-0.30	14.4	1	-5.81	23.5	-3.48	35.4	1
Dolomite (sedimentary)	-3.19	36.1	0.5	-7.36	52.2	-5.11	34.8	0.5
Dolomite (hydrothermal)	-3.76	56.7	0.5	-8.60	95.3	-5.37	45.7	0.5

We have chosen to implement this kinetics because differently from the model described by equation 4.12, its formulation does not hypothesize operating conditions as a gaseous phase of CO_2 at constant pressure in equilibrium with the system (David L Parkhurst, C. Appelo, et al. 1999). Moreover, in Palandri kinetic (equation 4.14), saturation state Ω is explicitly expressed as suggested by PHREEQC manual, so the effects of precipitation and dissolution are bound to saturation index (David L Parkhurst, C. Appelo, et al. 1999). Palandri and Kharaka work provides a common scheme describing the dissolution in water of different minerals, this makes it easier to compare the results among calcite and dolomite reactions in BAWL functioning.

4.2 Kinetic model validation

Busenberg and N. Plummer have obtained the rate equation 4.9 by testing dolomite dissolution in different condition, and then extrapolating the kinetics parameters of equation 4.9 (Busenberg and N. Plummer 1982). To assess the implementation of Palandri rate within PHREEQC, equation 4.14 is employed to reproduce the experiments described by Busenberg an Plummer, and then resulting rates are compared with that given by Busenberg and Plummer.

The experimental set-up can be outlined by some main features:

- A reactor of distilled water in which dolomite grains (with average initial surface area of 3 cm^2) are dispersed.
- A mixture of CO_2 and N_2 is bubbled into the reactor, so the solution is in equilibrium with the carbon dioxide gaseous phase and the reactor is well-mixed.
- The tests are conducted at constant pH, using a reagent such as HCl or KOH to stabilize it at a prescribed value.

The rates explicitly reported in Busenberg's work (Busenberg and N. Plummer 1982) refer to a limited sets of experiments compared to whole tests performed for the article, namely these results refer to two specific samples of dolomite: one hydrothermal and sedimentary. For hydrothermal dolomite, the experiments reported were conducted all at 25°C but with different pH and CO_2 pressure. Instead, the tests with sedimentary dolomite were performed at different temperature but with fixed pH and without CO_2 injection.

The results obtained with equation 4.14 are compared to these two sets of rates because more general rates are not reported.

To assess the general validity of Palandri rate implemented in PHREEQC, also the calcite dissolution kinetics is simulated with equation 4.14.

Rates obtained are compared with those calculated in the same condition with default calcite rate present in the software, equation 4.12, and with those reported in a work of Plummer et al., which studied the calcite dissolution as reported for dolomite and extrapolated the reaction rate 4.10 (L. Plummer, Wigley, and D. Parkhurst 1978).

4.2.1 Validation results

Dolomite kinetics

Tables 4.2 and 4.3 show respectively the simulations results of hydrothermal and sedimentary dolomite dissolution, calculated by equation 4.14 with PHREEQC. These obtained rates are compared with that reported in the work of (Busenberg and N. Plummer 1982). The results expressed as the negative base-10 logarithm of the rates in moles $\mathrm{cm}^{-2}\,\mathrm{s}^{-1}$, which means that at an higher value correspond a slower dissolution. The Figures 4.1, 4.2, 4.3, 4.4 and 4.5 report graphically the results.

Generally, the test performed in PHREEQC with Palandri's kinetic results in a slightly faster dissolution process then the one performed by Busenberg et al.

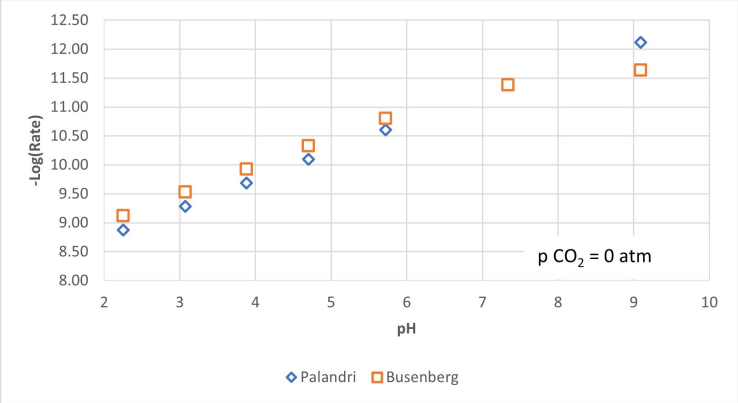

Figure 4.1: Comparison between hydrothermal dolomite dissolution rates, calculated by equation 4.14 (Palandri and Kharaka 2004) and compared with rates obtained by 4.9 in (Busenberg and N. Plummer 1982). Test performed at 25°C and without CO_2 injection.

Calcite kinetics

Table 4.4 reports the result of calcite dissolution simulations (rates expressed as the negative 10-base logarithm). The tests are performed within PHREEQC, with equation 4.14, from the work of (Palandri and Kharaka 2004), and with equation 4.12 the default kinetics model implemented in the software (David L Parkhurst, C. Appelo, et al. 1999). Both the models are compared with the rates calculated by equation 4.10, reported in (L. Plummer, Wigley, and D. Parkhurst 1978).

Table 4.2: -Log(Rate) of hydrothermal dolomite dissolution expressed in moles $\mathrm{cm}^{-2}\,\mathrm{s}^{-1}$, first three columns report the tests parameters utilized by (Busenberg and N. Plummer 1982), these results are compared to rates calculated by PHREEQC at the same conditions, with equation 4.14 (Palandri and Kharaka 2004).

T [°]	CO_2 [atm]	pH	Busenberg et al. 1982	Calculated eq. 4.14
25	0	2.25	9.12	8.87
25	0	3.07	9.53	9.28
25	0	3.88	9.93	9.69
25	0	4.7	10.33	10.10
25	0	5.72	10.80	10.61
25	0	7.34	11.38	11.39
25	0	9.09	11.64	12.12
25	0.003	3.92	9.92	9.71
25	0.003	4.18	10.03	9.84
25	0.003	4.54	10.18	10.02
25	0.003	5	10.36	10.25
25	0.29	2.9	9.35	9.20
25	0.29	3.57	9.59	9.53
25	0.29	4.6	9.87	10.05
25	0.29	4.2	9.77	9.85
25	0.958	2.01	8.94	8.75
25	0.96	2.54	9.15	9.02
25	0.965	3.4	9.43	9.45
25	0.966	3.68	9.50	9.59
25	0.96	4.22	9.63	9.86
25	0.96	5.2	10.17	10.35

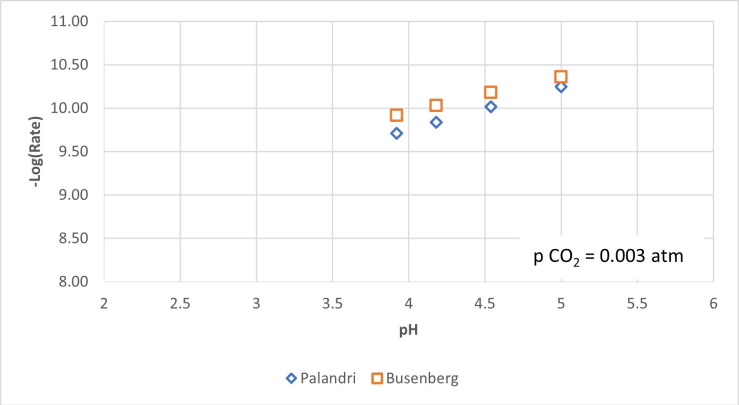

Figure 4.2: Comparison between hydrothermal dolomite dissolution rates, calculated by equation 4.14 (Palandri and Kharaka 2004) and compared with rates obtained by 4.9 in (Busenberg and N. Plummer 1982). Test performed at 25°C and 0.003 atm of CO_2.

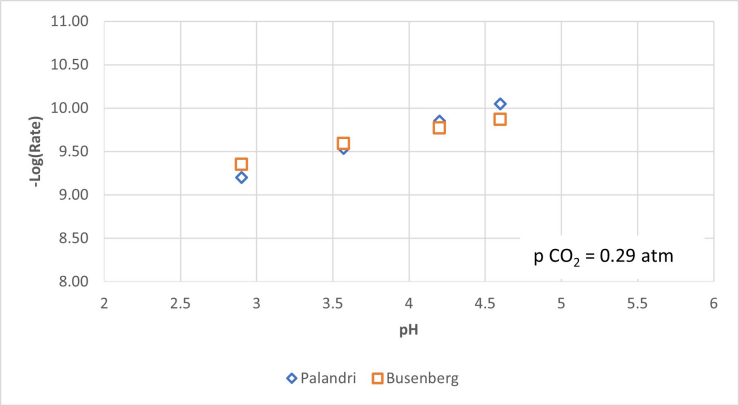

Figure 4.3: Comparison between hydrothermal dolomite dissolution rates, calculated by equation 4.14 (Palandri and Kharaka 2004) and compared with rates obtained by 4.9 in (Busenberg and N. Plummer 1982). Test performed at 25°C and 0.29 atm of CO_2.

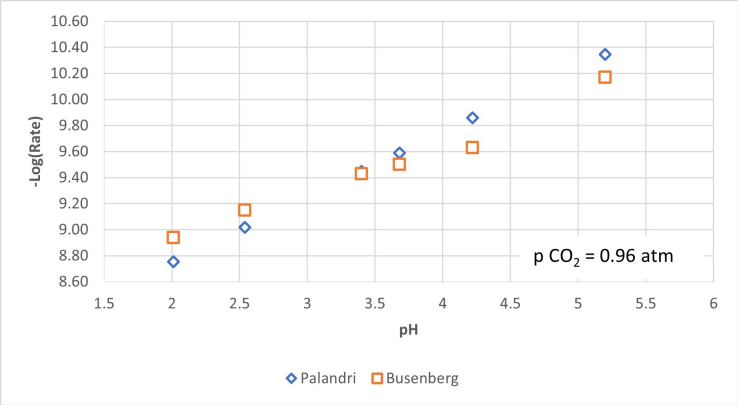

Figure 4.4: Comparison between hydrothermal dolomite dissolution rates, calculated by equation 4.14 (Palandri and Kharaka 2004) and compared with rates obtained by 4.9 in (Busenberg and N. Plummer 1982). Test performed at 25°C and 0.96 atm of CO_2.

Table 4.3: -Log(Rate) of sedimentary dolomite dissolution expressed in moles $cm^{-2}\,s^{-1}$, first three columns report the tests parameters utilized by (Busenberg and N. Plummer 1982), these results are compared to rates calculated by PHREEQC at the same conditions, with equation 4.14 (Palandri and Kharaka 2004).

pH	CO_2 [atm]	T [°]	Busenberg et al. 1982	Calculated eq. 4.14
3	0	5	9.58	9.14
2.99	0	15	9.29	8.90
2.96	0	25	8.96	8.66
2.95	0	35	8.73	8.45
2.95	0	45	8.60	8.26
3	0	55	8.33	8.11
2.98	0	65	7.93	

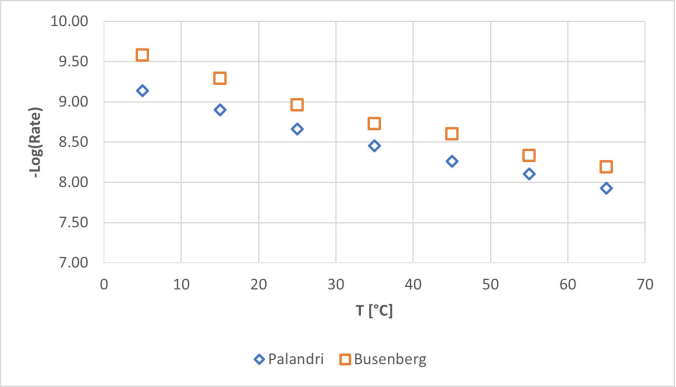

Figure 4.5: Comparison between sedimentary dolomite dissolution rates, calculated by equation 4.14 (Palandri and Kharaka 2004) and compared with rates obtained by 4.9 in (Busenberg and N. Plummer 1982). Test performed at different temperatures, pH≅3 and without CO_2 injection.

In Figure 4.6, 4.7 and 4.8 the different rates, show a good agreement (deviation under the 3%), except when the presence of CO_2 increases: here the rates calculated by equation 4.14 indicates a slower dissolution then the other two kinetics: the difference with other rates is about 9% when CO_2 phase is at 0.97 atm and pH is 6.

4.2.2 Validation discussion

Dolomite kinetics

The kinetics implemented show a good agreement with rates reported in articles (Busenberg and N. Plummer 1982) and (L. Plummer, Wigley, and D. Parkhurst 1978): the rates follow same trends and do not diverge more than 5%, a deviation that can occur naturally in dolomite.

It is important to highlight that, Busenberg and Plummer in their work have analyzed dissolution kinetics of different dolomite samples, and have extrapolated kinetics parameters (k_1, k_2, k_3, k_4) for each samples, then have calculated different values for average composition of sedimentary and hydrothermal dolomite (Table 4.5). Comparing the different rates constants calculated in the reference article for eight samples of dolomite (Table 4.5), it is clear that different samples do not dissolve at same velocity. Until now, In Tables 4.2 and 4.3 the reference rates used relate to the samples "Hydro 1" and "Sed 1" of Table 4.5 respectively for hydrothermal and sedimentary dolomite, which kinetics can give a slower dissolution compared to other samples.

Table 4.4: -Log(Rate) of calcite dissolution expressed in moles $\mathrm{cm}^{-2}\,\mathrm{s}^{-1}$, first three columns report the tests parameters utilized by (L. Plummer, Wigley, and D. Parkhurst 1978), these results are compared to rates calculated by PHREEQC at the same conditions, with equation 4.12 (David L Parkhurst, C. Appelo, et al. 1999) and equation 4.14 (Palandri and Kharaka 2004).

T [°]	CO_2 [atm]	pH	Plummer et al. 1978	Calculated 4.12	Calculated 4.14
25	0	2.0	6.5	6.29	6.30
25	0	3.0	7.45	7.29	7.30
25	0	4.0	8.25	8.28	8.29
25	0	5.0	9.25	9.20	9.18
25	0	6.0	9.5	9.77	9.69
25	0	7.0	9.75	9.90	9.80
25	0.3	2.0	6.5	6.29	6.30
25	0.3	3.0	7.4	7.29	7.30
25	0.3	4.0	8.25	8.25	8.29
25	0.3	5.0	9	9.01	9.18
25	0.3	6.0	9.4	9.39	9.69
25	0.97	2.0	6.5	6.29	6.30
25	0.97	3.0	7.25	7.28	7.30
25	0.97	4.0	8.15	8.20	8.29
25	0.97	5.0	8.75	8.76	9.18
25	0.97	6.0	8.9	9.03	9.69

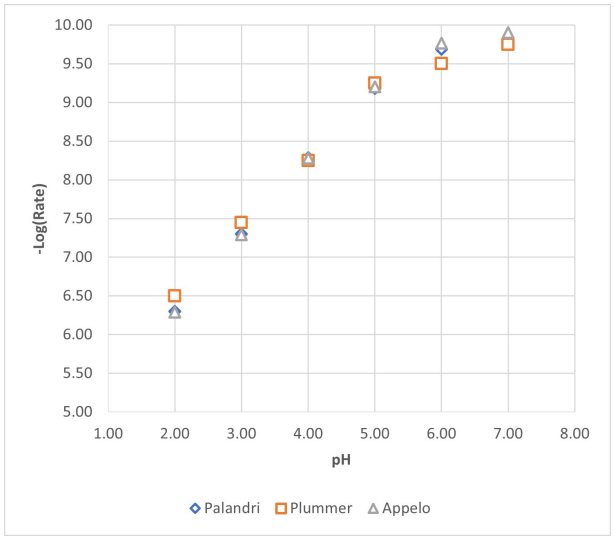

Figure 4.6: Comparison between calcite dissolution rates, calculated by equation 4.14 (Palandri and Kharaka 2004), and 4.12 (David L Parkhurst, C. Appelo, et al. 1999), and compared with rates obtained by 4.9 in (Busenberg and N. Plummer 1982). Test performed at 25°C and without CO_2 injection.

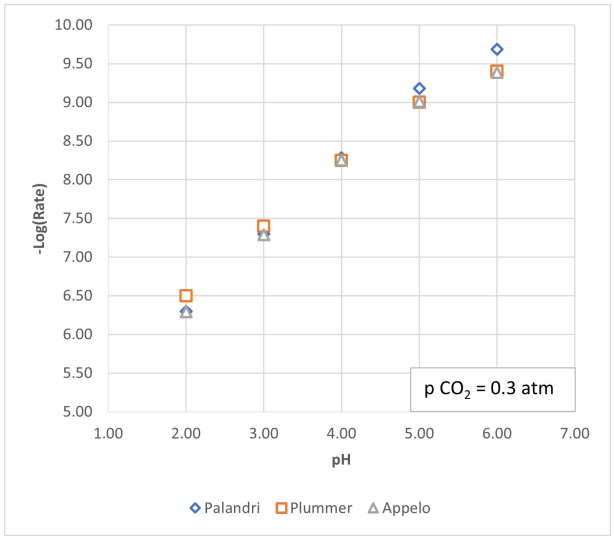

Figure 4.7: Comparison between calcite dissolution rates, calculated by equation 4.14 (Palandri and Kharaka 2004), and 4.12 (David L Parkhurst, C. Appelo, et al. 1999), and compared with rates obtained by 4.9 in (Busenberg and N. Plummer 1982). Test performed at 25°C and 0.3 atm of CO_2.

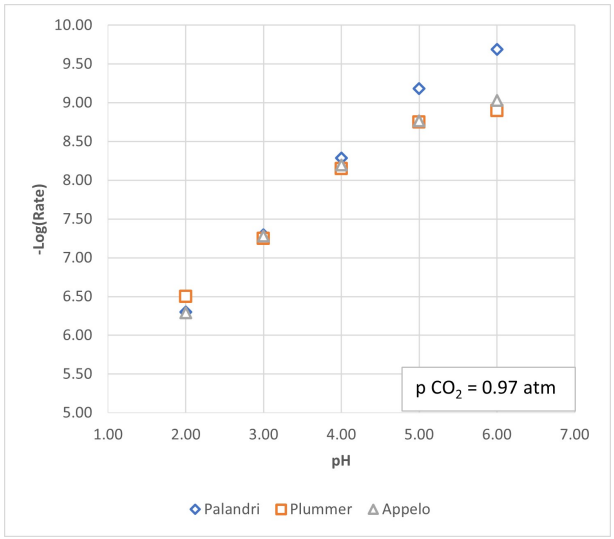

Figure 4.8: Comparison between calcite dissolution rates, calculated by equation 4.14 (Palandri and Kharaka 2004), and 4.12 (David L Parkhurst, C. Appelo, et al. 1999), and compared with rates obtained by 4.9 in (Busenberg and N. Plummer 1982). Test performed at 25°C and 0.97 atm of CO_2.

Figure 4.9 reports different dolomite rates value calculated with equation 4.9 for the samples analyzed by Busemberg and Plummer work. The rate constants (k_1, k_2, k_3, k_4) utilized are reported in Table 4.5, while the ions activities are fixed for each sample, as first approximation are obtained with PHREEQC simulating one specif test (hydrothermal dolomite dissolution at pH=3, CO_2 injected in the reactor at 0.97 atm). This approach is simplified but shows the percentage variation that dissolution rates can assume depending on different mineral samples; namely, the percentage value reported in Figure 4.9 refers to the rate variation on the samples "Hydro 1" and "Sed 1" used as references in Tables 4.2 and 4.3.

Rates calculate with equation 4.14 result acceptable if referred to a generic kind of dolomite, because they deviate from theoretical rates of (Busenberg and N. Plummer 1982) in the same range with which different dolomite sample deviate between them.

Calcite kinetics

In calcite analysis, it is evident that th main difference between equation 4.14 and equations 4.10, 4.12 is that Palandri and Kharaka rates do not account directly for CO_2 presence, and the rates implemented remain constant despite the CO_2 pressure changes. This is well visible in Figure 4.8: trends of reaction

Table 4.5: Kinetics constants reported by Busenberg et al. (Busenberg and N. Plummer 1982) at 25°C. Samples "Sed 1" and "Hydro 1" are the that considered for the assessment of dissolution rate (Tables 4.2 and 4.3). The voices "Average sedimentary" and "Average hydrothermal" refer to the mean value of rate constants that the authors have extrapolated for the rates uses.

Dolomite samples	k_1	k_2	k_3	k_4
Sed 1	3.39E-05	1.07E-06	2.40E-09	3.16E-05
Sed 2	3.16E-05	6.76E-07	3.39E-09	1.00E-05
Sed 3	6.76E-05	5.25E-07	1.51E-09	1.58E-05
Sed 4	4.07E-05	1.26E-06	5.01E-06	5.62E-05
Average sedimentary	6.52E-05	7.81E-07	2.98E-09	2.79E-05
Hydro 1	1.00E-05	9.33E-07	2.00E-09	5.62E-05
Hydro 2	1.91E-05	4.79E-07	4.79E-11	2.00E-05
Hydro 3	1.00E-05	4.27E-07	8.51E-10	5.01E-06
Hydro 4	2.09E-05	7.41E-07	2.24E-10	1.00E-05
Average hydrothermal	1.75E-05	4.31E-07	2.52E-10	2.79E-05

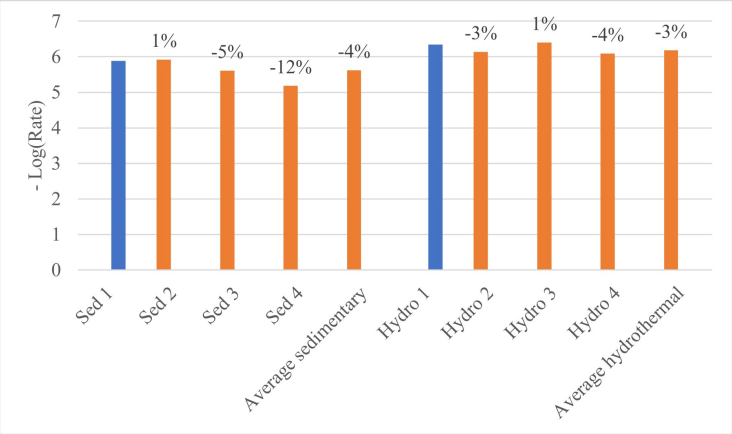

Figure 4.9: Comparison between dissolution rates of different dolomite samples. Those in blue are that took as reference in Tables 4.2 and 4.3. The labels refer to the percentage variation on these samples. Rate expressed as moles $\mathrm{cm}^{-2}\,\mathrm{s}^{-1}$.

diverge when CO_2 and pH increase, namely when the contribution of H^+ activity decreases compared to the other factor presents in the rate 4.10. Generally in calcite dissolution, the effects of pH, carbonate and bicarbonate ions (which presence depend on pH value) are more relevant that the presence of CO_2 (Pokrovsky, Golubev, and Schott 2005; Pokrovsky, Golubev, Schott, and Castillo 2009). In the Palandri and Kharaka model, the amount of carbon dioxide in the solutions is yet important because it significantly changes the pH and so it influences indirectly the mineral dissolution. However, in a test with fixed pH this influence is not appreciable because the acidity is modified artificially and the pH not depends on CO_2. It's also relevant to observe that in BAWL technology the levels of CO_2 in solution are not constant, but decrease in time thanks to the reaction with ${CO_3}^{2-}$ released by carbonate minerals. Therefore the rates difference tends to decrease in time and the lack of consideration of CO_2 observed in equation 4.14 is gradually less significant.

4.2.3 Validation conclusions

Equation 4.14 results suitable in the PHREEQC software, and appropriate for our purpose, because:

- The usage of a same kinetics model for different minerals facilitates the rate comparison between dolomite and calcite dissolution.
- Palandri and Kharaka model does not hypotheses set-up conformation, as the equation 4.12 that for example suppose a system of pure water, calcium and CO_2.
- The deviations of Palandri rates compared to the ones found by (Busenberg and N. Plummer 1982; L. Plummer, Wigley, and D. Parkhurst 1978) are in acceptable ranges. Namely, the deviation of dolomite and calcite rates from the reference rates are in range valid also for different minerals samples.

For these reasons, the following simulation on BAWL technologies were performed using the equation 4.14 for calcite and dolomite dissolution.

4.3 Mineral dissolution rate comparison

In literature, different works analyze and compare the dissolution rates of various carbonate minerals as dolomite, calcite and magnesite (L. Chou, Garrels,

and Wollast 1989; Z. Liu, Yuan, and Dreybrodt 2005). Calcite results a mineral characterized by a fast-dissolution kinetics, and this is confirmed also in our work (Figure 4.10).

It is important to highlight that calcite and dolomite have different content of carbonate ions. In reactions 4.1 and 4.2, it is evident that one mole of dolomite releases two moles of carbonate ions when dissolved, while calcite only one. So, the dissolution rates can express in moles of carbonate ions released in the solution: calcite rate does not change, but dolomite rate increases. This different expression of the rates decreases the differences between calcite and dolomite dissolution, but the calcite reaction remains faster.

Since dolomite is generally less soluble than calcite, its application in BAWL might be more difficult. For this reason, in the following section, only the sedimentary dolomite is applied to BAWL; if its employment on BAWL will not involve difficulties, the hydrothermal dolomite will be taken into account.

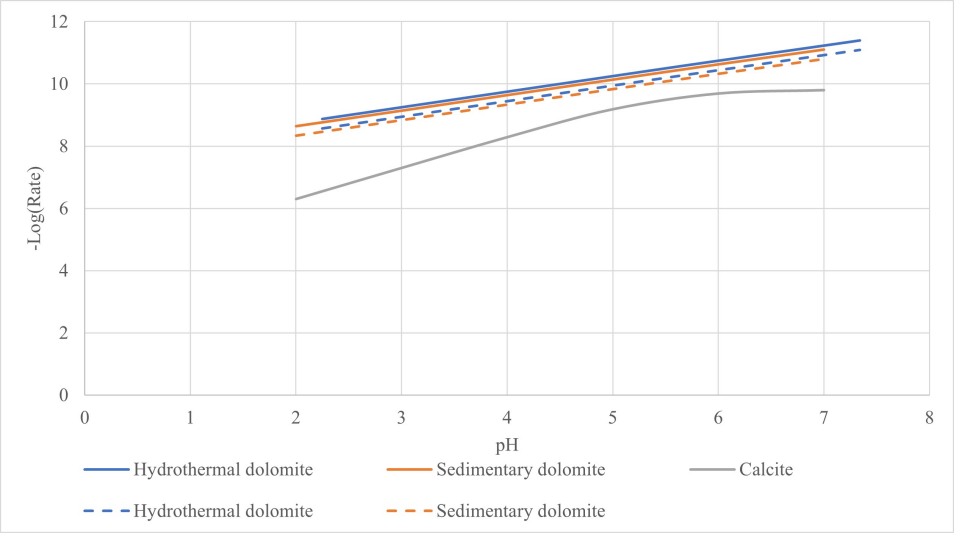

Figure 4.10: Dolomite and calcite rate comparison, the solid line refers to rate expressed as moles of mineral dissolved, while the dashed refers to dissolution expressed as moles of carbonate ion released. Rate expressed as moles $\mathrm{cm}^{-2}\,\mathrm{s}^{-1}$.

Chapter 5

BAWL working conditions

This chapter aims to assess different feasible working conditions for BAWL. The first section examines the variables that influence the dissolution rate (equation 4.12) and bounds these variables to the operating parameters of the BAWL technology. Namely, the functional aspects of the BAWL that are controllable during the BAWL application.

Then, based on previous work (Caserini et al. 2021), we have assigned some starting value to BAWL parameters, as pipeline length, discharge depth etc. A first sensitivity analysis is performed on this starting value to determine which parameters influence the most the functioning of BAWL, in this study, the parameters are all varied by the same percentage value. Since each parameter has its feasible range of values, another analysis is performed in which the values of the range are due to the effectiveness parameters variability.

After identifying the most influential parameters in their feasibility range, they are combined to determine different feasible working points. Among the working condition suitable for BAWL are identified operating points that optimize different parameters. These points will be the ones recommended for BAWL working.

- Carbonate mineral must be all dissolved at the end of pipeline, to prevent obstruction of the DR pipe or accumulation of unreacted material on the seabed, and do not waste materials.
- The consumption of carbon dioxide by calcite should be maximized as far as possible, to limit the use of calcium hydroxide.
- The depth and length of the pipeline should be minimized so as to increase the practical feasibility of BAWL, taking care not to compromise the overall efficiency of the system.

5.1 Parameters presentation

The variables that influence directly minerals and dissolution rate 4.14 are:

- Saturation index.
- Temperature.
- Activity of hydrogen ions.
- Specific surface area of the mineral.
- Reaction time.

Saturation index Saturation index SI is a parameter that indicates how much the solution is near the saturation.

$$SI = log_{10}\Omega = log_{10}\frac{IAP}{K} \tag{5.1}$$

IAP is the Ion Activity Product, calculated by the product of mineral ions activities effectively present in the solution. At the same time, K is the solubility product, obtained as the IAP but considering ions activities at the equilibrium. For example, IAP and K of calcite are calculated as reported in equations 5.2 and 5.3; the subscripts specify if the ions activities relate to equilibrium or at a specific time t.

$$K = (a_{CO_3^{2-}})_{eq}(a_{Ca^{2+}})_{eq} \tag{5.2}$$

$$IAP = (a_{CO_3^{2-}})_{t}(a_{Ca^{2+}})_{t} \tag{5.3}$$

When SI is equal to 0, the mineral phase and the solution are respectively in equilibrium. If SI is higher or lower than 0, the solution can be respectively supersaturated or undersaturated. In applying BAWL, the saturation state of the mineral should remain considerably under 0, because otherwise the dissolution reaction will be too slow and not completed.

Ion activities depend on compound concentration, temperature and pressure, so the saturation index also depends on these variables. Namely, the SI diminish with an increase in pressure and decrease of temperature and concentration.

Temperature It influences dissolution rate in two ways: a higher temperature speeds up the dissolution rate (see equation 4.14), but simultaneously, it entails a less favourable SI for minerals. So, we can expect that a higher temperature is preferable when SI contributes less to the dissolution process, so solutions are far from saturation.

Commonly, ocean temperatures change with the increase of depth (Robinson and Stommel 1959). As an example, the Mediterranean sea temperature decreases almost linearly in the first section (approximately until 100 m of depth), and then sea temperature stabilize (Houpert et al. 2015).

Temperature is the parameter that, in this work, will be less investigated because, among the other parameters, it is the one on which we have less control because the changing temperature of a large amount of water will be too energy-expensive. The only way to influence this parameter is to change the depth at which supply water.

Activity of hydrogen ion Hydrogen ions are one of the main factors influencing the dissolution rate, which is composed of three mechanisms distinct from pH solution.

The natural pH of seawater is about 8. For example, in the Mediterranean sea, the pH varies from 8 at 2500 meters to 8.10 at 100 meters of depth; these data are provided by CMCC (Centro Mediterraneo sui Cambiamenti Climatici) (Butenschön, 2021 - personal communication).

From figure 4.10, it can be understood the importance of a low pH: the dissolution rate of calcite decreases rapidly at pH higher than 6-7. In the application of BAWL, the injection of CO_2 is fundamental to lower the pH and achieve a complete consumption of the mineral. Therefore, it can be advantageous to dose carbonate minerals and CO_2 with a sub-stoichiometric molar ratio: the pH will be favourable until the mineral is not all reacted, and then the residual carbon dioxide will be neutralized by the addition of $Ca(OH)_2$.

In practice, the activity of hydrogen ions is strongly influenced by the molar ratio between carbon dioxide and minerals and by the amount of water used to dissolve CO_2.

Specific surface area of the mineral The reaction area is directly influenced by the size of mineral grains, which is mainly described by the diameter of the particles.

The surface area of minerals is crucial for dissolution speed. If a solid mineral is divided into small particles, the specific surface is maximized, and it will be dissolved easily by water.

It is important to stress that the size of the grains does not influence the total amount of minerals that can dissolve in a solution but the speed of dissolution. pH and SI determine the amount of calcite that can be dissolved, but a low mineral specific surface increases the time required. Such an increase could not be suitable for BAWL applications.

Reaction time To have a complete dissolution, the reaction must have enough time to develop, so have at disposal a higher amount of time is preferable. However, it is essential to remember that if the saturation index approaches zero, the dissolution rate will be too slow, and it won't arrive at a complete dissolution in a feasible time for the technology.

We can modify reaction time by changing the period in which the solution remains in the pipeline (the reactor). Having to maintain a minimum velocity in the pipeline to prevent the sedimentation, the physical properties that we will control is the pipeline's length.

From these observation, we can highlight the specific feature of BAWL technology on which we can act:

- Molar ratio between minerals and CO_2.
- Consumption of water.
- Diameters of minerals particles.
- Length of the pipeline.
- Depth of the pipeline.

Table 5.1 summarizes the connection between rate variables and technology feature. The arrows show if the variables should increase or decrease to speed up the dissolution reaction and how the technology parameters influence the rate variables. For example, high activities of hydrogen ions speed us the kinetics, and to generate this beneficial effects on the hydrogen ions activity, molar ratio and water consumption should be low. Increasing water usage will act positively on the saturation index but negatively on the activities of hydrogen ions.

5.2 Parameters range

In this section, the technology parameters are analyzed and are identified some range of values in which they could vary.

Table 5.1: Recap of which technology parameter can influence the rate variables in an advantageous way for the functioning of BAWL. The arrows indicate if the rate variables should increase or decrease to speed up the dissolution and how the technology parameter should vary to generate the beneficial effect on the corresponding variable.

Rate variables	Technology parameters
Activity of hydrogen ion ↑	Molar ratio ↓ Water consumption ↓
Reaction area of the mineral ↑	Diameter of the grains ↓
Saturation index ↓	Depth of the pipeline ↑ Molar ratio ↓ Water consumption ↑
Reaction time ↑	Length of the pipeline ↑

Molar ratio Equation 3.4 defines the stoichiometric ratio between calcite and CO_2 as 1:1, but it can be advantageous to reduce this molar ratio and have a lower amount of $CaCO_3$ compared to CO_2. However, this ratio cannot be too small because otherwise, at the end of the pipeline, we will have a pH too acid, which involve high consumption of $Ca(OH)_2$.

To evaluate an optimum moral ratio, we have analyzed a range from the stoichiometric value 1 to 0.1, which means that calcite dosed is one-tenth of the stoichiometric quantitative.

Depth of pipeline - Pressure The final depth that the pipeline reaches should be minimized as possible because to pose at a high profundity in the ocean requires a significant engineering effort. Moreover, not all the seafloors arrive at a depth of 3000 km (290 atm) in the coast's proximity. Nevertheless, pressure influences saturation index, speeding up the reaction and helps to avoid CO_2 degassing: so it should not be too low.

The pressure range considered is $50 \div 300$ atm, which correspond to depths of $516 \div 3100$ meters (given that the pressure increase of 1 atmosphere every 10.33 meters of depth).

Grain diameters The specific surface area of mineral grains is calculated as follow:

$$SA = \frac{M}{\rho}\frac{3}{r} \tag{5.4}$$

Where:

- SA: specific surface area ($cm^2\,mol^{-1}$).

- M: molar mass of carbonate mineral, 100.09 $g\,\mathrm{mol}^{-1}$ for calcite and 184.40 $g\,\mathrm{mol}^{-1}$ for dolomite.
- ρ: minerals densities, assumed as 2.762 $g\,\mathrm{cm}^{-3}$ for calcite and 2.915 $g\,\mathrm{cm}^{-3}$ for dolomite (Gattinoni, Papini, and Scesi 2002).
- r: radius of the grains (cm).

The specific surface of the grain changes along dissolution proportionally to the relationship between initial and actual moles of reactant (C Anthony J Appelo and Postma 2004).

$$Area = SA \cdot n_0 \Big(\frac{n}{n_0}\Big)^{\alpha} \tag{5.5}$$

Where:

- $Area$: adjusted value of the specific surface area ($\mathrm{cm}^2\,\mathrm{mol}^{-1}$).
- n_0: initial moles of minerals (mol).
- n: actual moles of unreacted minerals (mol).
- α: correction factor, assumed as 0.6 (Larsen and Postma 2001).

This formulation is theoretically suitable only for idealised particles distribution. Namely, the mineral grains should be all spherical, and the distribution of particles should be mono-dispersed. Usually, these assumptions are not verified in practice, but the use of equation 5.5 shows a good agreement with empirical data (C Anthony J Appelo and Postma 2004). Moreover, the miller allows to reach particles distribution with D90 of the desired size (see Figures 5.1 and 5.2).

Currently, the industrial milling process allows reaching of particles diameters of about 2 μm In the thesis, particles with diameters of 10, 5 and 2 μm are considered to evaluate which size of the particles is most suitable for BAWL.

Length of pipeline Fixed at 1.2 ms^{-1} the minimum flow speed that avoids sedimentation in the pipeline, length is calculated thanks to the time that minerals need to dissolve completely.

$$Length = v \cdot t \tag{5.6}$$

As a first approximation, the pipeline is set as 120 km, as the maximum amount of time that the reaction can employ to dissolve completely is 100,000 seconds (27.8 hours). If the mineral dissolution is completed before, the pipeline length is recalculated accordingly.

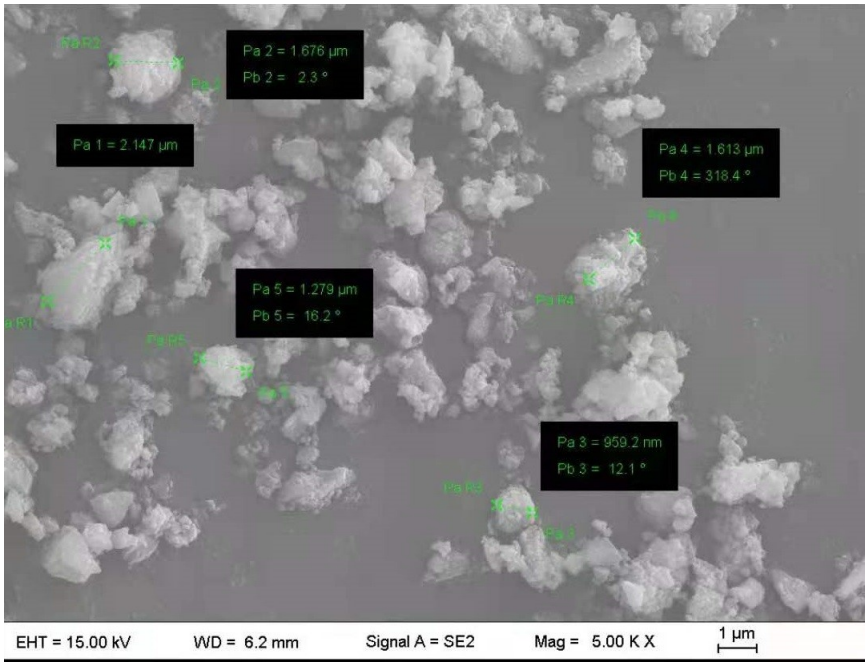

Figure 5.1: Microscopic photo of calcite, of distribution with D90=2 μm. Data provided by private industry.

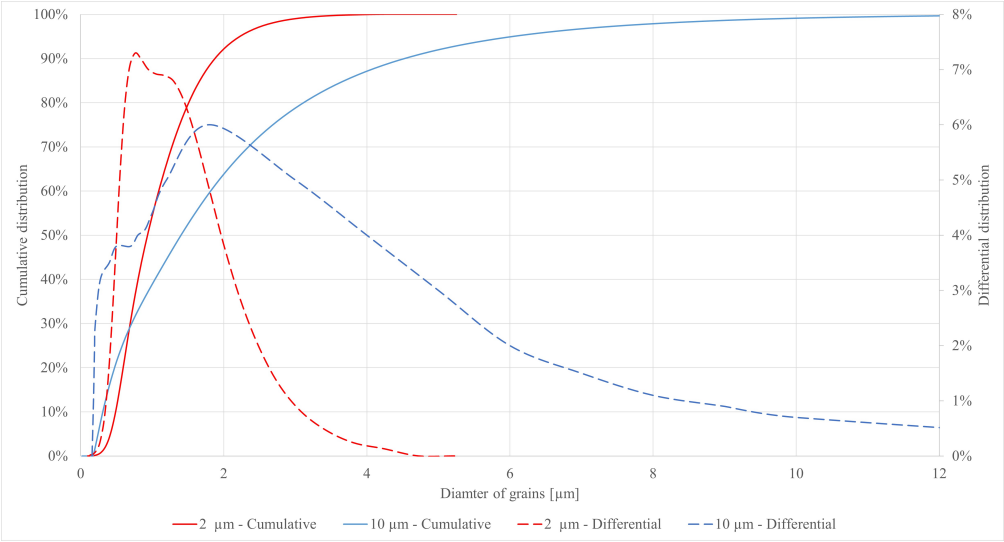

Figure 5.2: Graphic that shows obtenible cumulate and differential distribution for a milling processes aimed to obtain 2 μm and 10 μm size particles. Data provided by private industry.

Water usage It is quantified as the amount of water required for the dissolution of 1 CO_2 tonne. Regarding costs and environmental impact, this amount should be lower as possible, but a volume of water too small leads faster to the solution's saturation. Additionally, we have observed that diluting excessively CO_2 is counterproductive because solution acidity will be too low, and the mineral will not dissolve completely. As an example, Table 5.2 reports the pH obtained dissolving 1 tonne of carbon dioxide in different seawater volumes: increasing water, the pH decreases. In the functioning of BAWL, the progressive dissolution of carbonate minerals increases the pH to a value that will not allow the mineral dissolution.

We consider a volume of 2000 m^3 for CO_2 tonne, as has been done in previous works on BAWL (Cappello et al. 2021; Caserini et al. 2021).

Table 5.2: Resulting pH after the dissolution of 1 tonne of CO_2 in different seawater volumes, at T=16°C, initial pH=8. Data simulated with software PHREEQC.

Water volume [m^3]	pH
500	4.899
1000	5.166
1500	5.342
2000	5.468
2500	5.565
3000	5.645

5.3 Sensitivity analysis

To identify which parameter influence the most the BAWL functioning, a sensitivity analysis is performed on the specified parameters (here listed) that affect carbonate minerals dissolution.

- Water usage.
- Molar ratio.
- Reaction time.
- Initial temperature.
- Final pressure.
- Grains diameter.

The starting conditions are defined in the following section, then each parameter is varied by 1%. Then, with PHREEQC, the functioning of BAWL is simulated. Each parameter variation leads to a different final condition of the solution discharged. To compare the impact of each parameter on the overall efficiency of BAWL, it has been examined the dissolution of carbonate mineral achieved at discharge point because its complete dissolution is essential for the functioning of BAWL.

5.3.1 Base cases definition

To perform a sensitivity analysis, it is fundamental to define a base case. We have defined the seawater composition (Table 5.3) and the starting values of BAWL parameters as explained in section 5.1 (Table 5.4).

Table 5.3: Mineral composition of seawater (Lyman and Fleming 1940), the data are give as grams of salt present in a kilogram of seawater.

Mineral	grams of salt
Cl	18.9799
SO_4	2.6486
Br	0.0646
F	0.0013
Na	10.5561
Mg	1.272
Ca	0.4
Sr	0.0133
K	0.38

The final conditions of the seawater are reported in Table 5.5, where are showed the reduction of carbon dioxide and calcite, the pH of the solution and the saturation index of the carbonate minerals (calcite and dolomite). SI of calcite is -0.05, which indicate that the discharged solution is saturated; therefore, calcite and seawater are almost in equilibrium. But calcite is well far to complete dissolution because only 65.8% of the carbonate mineral is dissolved: and in this condition, having a complete dissolution will be difficult: even increasing the time at 300,000 seconds (about 83 hours), the calcite dissolution proceeds at 66.9%.

It can be interesting to verify how the different parameters act depending on the proximity to equilibrium when SI is not limiting the reaction. Therefore, in the sensitivity analysis, another base case is introduced, in which SI of the final solution is far from 0.

Table 5.4: Parameters value used for the preliminary simulation on BAWL. Temperature data are provided by CMCC (Centro Mediterraneo sui Cambiamenti Climatici) (Butenschön, 2021 - personal communication).

Parameter	Value
Mineral used	Calcite
Initial CO_2 [tonne]	1
Water usage [m^3]	2000
Molar ratio	Stoichiometric
Residence time [s]	100,000
T_0 [°C]	16
T_f [°C]	9
Pressure [atm]	290
Grains diameter [μm]	10

Table 5.5: Final condition that are obtained at the end of pipeline in the preliminary simulation on BAWL.

Parameter	Value
CO_2 reduction	65.81%
Mineral reduction	65.34%
pH	6.63
SI $CaCO_3$	-0.05
SI $CaMg(CO_3)_2$	0.53

As reported in section 5.1, SI is influenced by the depth of the pipeline, molar ratio, and water usage. A reduction of the molar ratio acts favourably on the saturation index and hydrogen activity (Tabel 5.1), so the second base case changes from the first because the carbonate mineral is dosed half of the stoichiometric.

Sensitivity analysis is performed on two different base cases:

- Saturated (S): mineral and carbon dioxide is dosed stoichiometrically. The discharge solution reach condition near saturation; further carbonate minerals dissolution is difficult to achieve.

- Not Saturation (NS): molar ration between mineral and carbon dioxide is sub-stoichiometrical (0.5:1). The discharge solution is far from saturation; further dissolution of carbonate minerals is difficult to achieve.

Table 5.6 reports the parameter values setting for each base case.

The BAWL functioning is simulated within PHREEQC, with calcite and dolomite as carbonate minerals. Table 5.7 reports the condition that seawater assumes at discharge point on the different base cases.

It's important to highlight that setting the same initial condition for dolomite and calcite will not lead to the same saturation grade of the solution. Calcite and dolomite kinetics proceed at distinct speeds, so the amount of mineral dissolved will be different after the same time, and so the saturation grade. Namely, at "S" condition, the SI of dolomite and calcite are -0.16 and -0.05 respectively.

In each simulation, SI of calcite and dolomite are monitored, despite the minerals applied, because it is essential to ensure that no carbonate minerals will precipitate. In BAWL simulations, the dolomite saturation is higher than calcite because of the abundance of magnesium present in seawater (Table 5.7). Moreover, dolomite has a positive SI in the dissolution of calcite, but it is not enough to generate precipitation in seawater (Morse and He 1993).

The sensitivity analysis performed are four, two on the dolomite and two on the calcite dissolution. In each study, the values of Table 5.6 are increased and decreased by 1%, and then the reduction of the mineral is compared with the one reported in Table 5.7. We have not explicitly compared the carbon dioxide reduction or other parameters as pH because it is consequent to mineral dissolution; to achieve complete degradation of the mineral is crucial for BAWL functioning.

Table 5.6: Starting value of the parameters for sensitivity analysis. NS and S indicate respectively the conditions that lead to a Not Saturated or Saturated solution.

	NS	S
Initial CO_2 [tonne]	1	1
Water usage [m^3]	2000	2000
Molar ratio	0.5	Stoichiometric
Residence time [s]	100,000	100,000
T_0 [°C]	16	16
T_f [°C]	9	9
Pressure [atm]	290	290
Grains diameter [μm]	10	10

Table 5.7: Final condition that are obtained at the end of pipeline in the different base cases. NS and S indicate respectively the conditions that lead to a Not Saturated or Saturated solution.

	Dolomite		Calcite	
	NS	S	NS	S
CO_2 reduction	40%	52%	49%	66%
Mineral reduction	79%	53%	98%	65%
pH	6.2	6.4	6.4	6.6
SI $CaCO_3$	-0.79	-0.47	-0.47	-0.05
SI $CaMg(CO_3)_2$	-0.77	-0.16	-0.26	0.53

5.3.2 Results and discussion

Table 5.8 and Figure 5.3 reports the percentage variation on mineral dissolution. This is calculated by the percentage reduction of carbonate minerals achieved in the base cases (Table 5.7) and the one obtained in the sensitivity analysis after the parameter variation.

In "S" conditions, increasing pressure and water volume can significantly enhance the dissolution because it acts on saturation state. But we see that these two variables assume less significance if the solution is far from equilibrium.

In the NS simulations, the more relevant parameters are grains diameter, reaction time and molar ratio.

The variation of temperature is complex to describe because of the double effect that it has on the kinetics. For calcite dissolution, the temperature does not influence the dissolution efficiency substantially. But for dolomite reaction, the temperature influence is more evident.

In all the cases analyzed, the molar ratio is one of the main parameters that can affect minerals dissolution: decreasing the mineral dosage of 1% increases its consumption of $0.8 \div 0.9$ % when the solution is near saturation. In Table 5.7 we can see that in "S" tests, the mineral dissolution is around $53\% \div 65\%$ (depending on minerals). The most effective way to increase its dissolution is to decrease the mineral dosage and move to "NS" condition (Table 5.8). Another way is to increase water usage and pressure, but use 2000 m^3 on CO_2 tonne and discharge the seawater at 290 atm (3000 m) is yet a big engineering effort. It is possible to conclude that BAWL should work in conditions that guarantee that the seawater solution will remain far from equilibrium. Namely, for the functioning of BAWL should be used an excess of CO_2 and planned to use calcium hydroxide to neutralize the residual acidity.

5.4 Sensitivity analysis - calcite

Each parameter has different range of feasible values, so it is interesting to assess the results variation in function of the effective parameters values that we will treat.

Starting from the base case "NS", reported in Table 5.6, one parameter is varied at a time with other effectively possible values. The amount of CO_2 dissolved in the starting solution is always 1 tonne.

Table 5.8: Results of the sensitivity analysis expressed as percentage variation of the reduction of the mineral. The percentage is calculated by dividing the difference between the new mineral dissolution achieved at the end of the simulation and the ones achieved in the base cases by the mineral dissolution of the base case. NS and S indicate respectively the conditions that lead to a Not Saturated or Saturated solution.

	Dolomite		Calcite	
	NS	S	NS	S
Water -	0.02%	-0.20%	-0.03%	-0.25%
Water +	-0.02%	0.19%	0.03%	0.25%
Molar ratio -	0.32%	0.87%	0.14%	0.93%
Molar ratio +	-0.32%	-0.86%	-0.15%	-0.92%
Residence time -	-0.33%	-0.09%	-0.12%	-0.04%
Residence time +	0.32%	0.08%	0.12%	0.04%
Temperature -	-0.16%	-0.01%	-0.03%	0.01%
Temperature +	0.16%	0.00%	0.03%	-0.01%
Pressure -	-0.06%	-0.16%	-0.02%	-0.15%
Pressure +	0.06%	0.16%	0.02%	0.15%
Grains diameters -	0.33%	0.08%	0.12%	0.04%
Grains iameters +	-0.33%	-0.08%	-0.12%	-0.03%

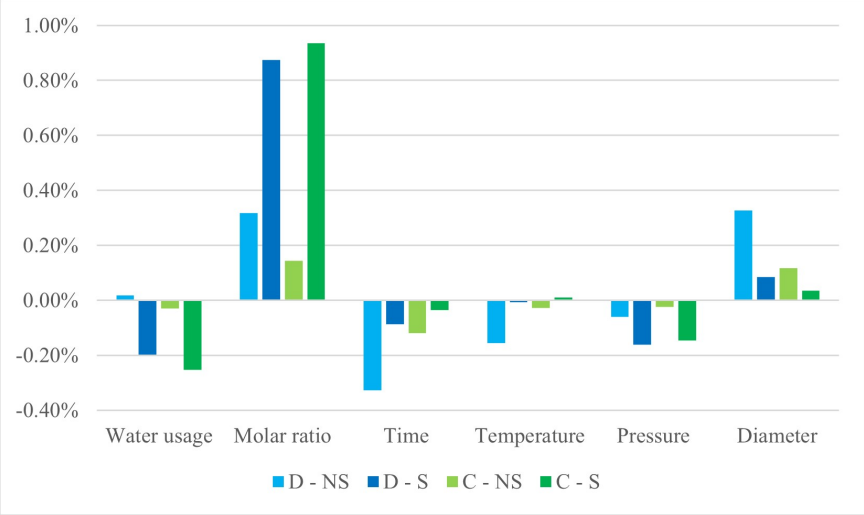

Figure 5.3: Histogram reporting results of the sensitivity analysis expressed as percentage variation of the reduction of the mineral. The figure reports only the variation of mineral reduction efficiency after the 1% parameters decrease.

Water usage

The consumption of water is not modified because, as seen in Table 5.8 it has little effect on dissolution (at "NS" condition). Moreover, to increase the dissolution, the water usage should be increased too, but this will reduce the storage capacity of the BAWL, as explained in chapter 6.

Molar ratio

The calcite is the main parameter that allows a complete calcite dissolution (Table 5.8), so it is examined in a wide range of values, namely from 1 to 0.1. Even if it is unlikely that BAWL will work a dose of calcite as one-tenth of CO_2 because it will involve an important reduction of the efficiency.

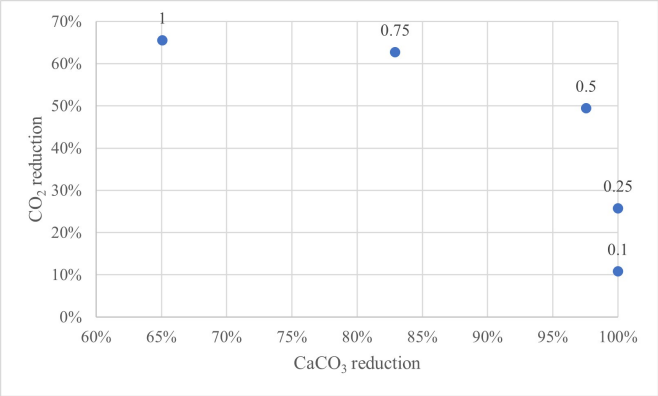

Figure 5.4: Calcite and carbon dioxide reduction in function of molar ratio.

Decrease the molar ratio leads to 0.25:1 ($CaCO_3$:CO_2) lead to a complete dissolution of calcite, but the reduction of CO_2 is highly reduced (Figure 5.4).

Reducing the molar ratio from 0.75 to 0.5 entails a variation in calcite and CO_2 reduction of the 15% and the - 13%, respectively. So the advantages in calcite dissolution are more than the disadvantage in CO_2 consumption. At the same time, there is no reason to reduce the molar ratio from 0.25 to 0.1 if the dissolution is yet completed at 0.25 because it will lead only to a reduction in CO_2 reaction and an increase of $CaCO_3$ requirement.

The optimal molar ratio value could be around 0.5. If a molar ratio of 0.5 the calcite dissolution is about 98%, the $CaCO_3$ can react completely by modifying other parameters.

Reaction time

The reaction times considered going from 50,000 seconds (14 hours) to 150,000 (42 hours) seconds. In the base case, we have supposed a starting time of 100,000 s, which entail a long pipeline yet, with the high cost and engineering effort, time parameter results relevant in sensitivity analysis, so we have tried to increase it until 150,000 seconds.

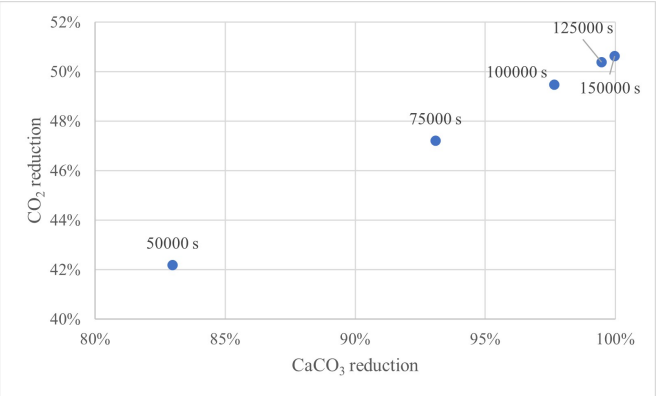

Figure 5.5: Calcite and carbon dioxide reduction in function of the residence time of the solution in the pipeline.

Increase the time lead to an increase of the calcite and CO_2 reduction (Figure 5.5). Increasing the residence time by 50% from 100,000 to 150,000 seconds gives a rise of 2% of calcite reduction, while the same increase from 50,000 to 100,000 seconds increases the efficiency of calcite reaction by 15%. That is because the dissolution rate decrease in time, for the increase of pH and SI. Considering that in length, 500,000, 100,000, and 150,000 seconds means pipeline of 60, 120, and 180 kilometers. Increase the residence until the 150,000 seconds of residence time does not seem worthy, but other parameters should be considered to assess it.

Initial temperature

In the Mediterranean sea, the surface temperature of the sea varies from 13 to 20°C (Houpert et al. 2015). So, in the analysis, the temperature range goes to 10 from 20°C.

The final temperature that the solution will reach is the one present at the discharge point. Still, this temperature does not vary under the 150 m of depth (Houpert et al. 2015), so its variation has not been investigated.

An increase of the surface temperature increases both calcite and CO_2 reduction (Figure 5.6). Unlike the other parameters which values are due to

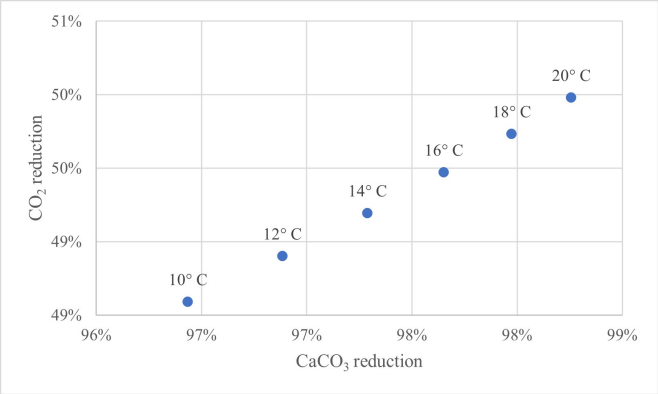

Figure 5.6: Calcite and carbon dioxide reduction in function of the initial temperature.

technological feasibility, the temperature range is bound to the characteristics of the Mediterranean sea. The maximum increase of calcite is about 2% when the temperature goes from 10 to 20°C.

The surface temperature affects less the calcite dissolution compared to other parameters as molar ratio and residence time (as already suggested by the sensitivity analysis, see Table 5.7).

Final pressure

The sensitivity analysis assess that the pressure gives a limited contribution in the NS cases, so this parameter is studied with lower value that the starting one, to enhance BAWL applicability.

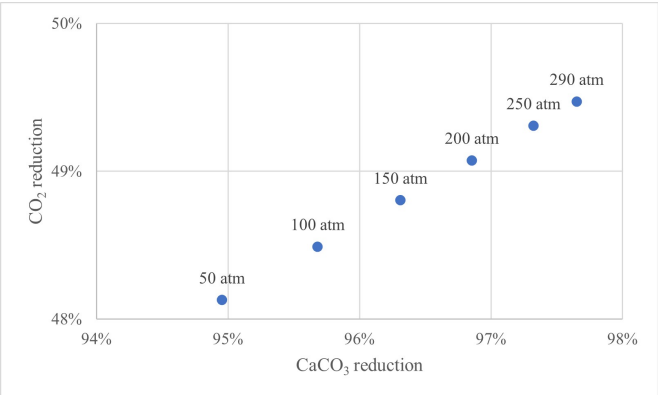

Figure 5.7: Calcite and carbon dioxide reduction in function of final discharge pressure.

Figure 5.7 shows that a substantial decrease in the discharge pressure reached by the pipeline reduces the system efficiency slightly. Namely, reducing the pressure from 290 to 50 atm (about 83%) lead to a decrease of 2.7%. The feasibility of BAWL increases drastically if the pipeline could reach 516 meters of depth instead of the 3000 m initially considered.

Nevertheless, this decrease in efficiency should be balanced by other parameters.

Grains diameter

The grains diameters analyzed goes from the starting value of 10 μm up to 2 μm, particles size currently commercialized.

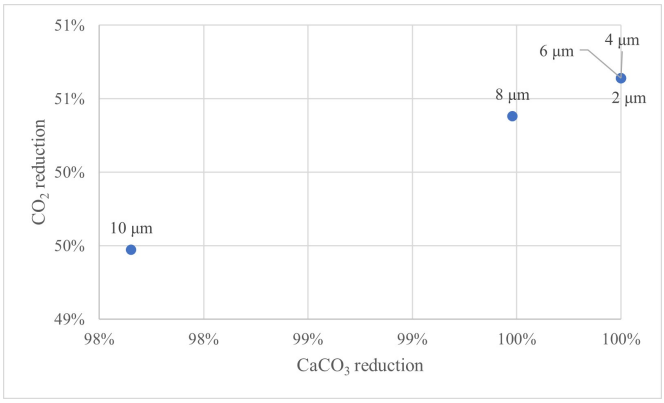

Figure 5.8: Calcite and carbon dioxide reduction in function of diameters of the grains.

Decreasing the size of the grains increase effectively the calcite dissolution (Figure 5.8). Namely, in the working conditions of the "NS" base case, chancing the diameter of the grains to 6 μm already allow complete dissolution of calcite, without decrease the CO_2 reduction, as for the molar ratio, or involve a longer pipeline, as for residence time.

Figure 5.9 reports all the parameters variation analyzed in one diagram, which shows that enhance one parameter among molar ratio, residence time and diameters of the grains can allow the complete dissolution of calcite. So, molar ratio, residence time and diameters of the grains are the most influential parameter to investigate to achieve complete dissolution of the calcite. However, it is essential to highlight that the increase of the residence time will lower the feasibility of BAWL; for this reason, in the following section, the focus is on the calcite molar ratio and size of the particles.

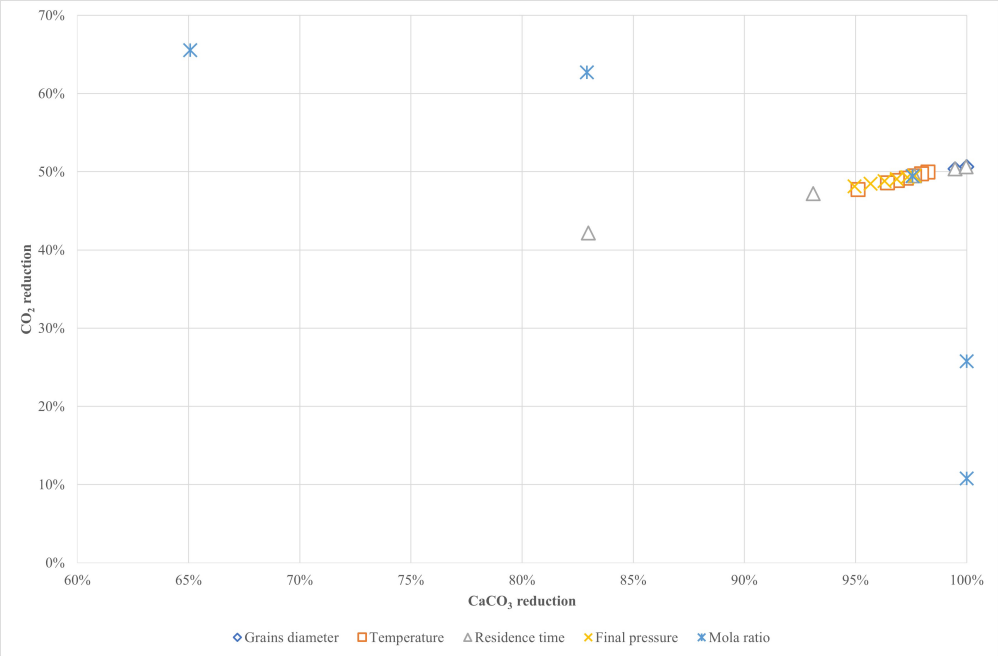

Figure 5.9: Calcite and carbon dioxide reduction in function of the different parameters.

The results given by the pressure are promising because decreasing the pressure at 50 atm lead to a decreasing in the dissolution of the 2.8 %, a gap that other parameters can overcome.

The following section combines different values to assess if particles diameter and molar ratio can improve the feasibility of the BAWL (e.g. reducing the pipeline depth).

Molar ratio, grains diameter and pressure combination

To understand how the size of the particles and the molar ratio can increase the efficiency of the BAWL, which functioning is simulated over different parameter combinations, reported in Table 5.9. Namely, molar ratio from 1 to 0.1 are combined with particles of 10, 5 and 2 μm; this set of simulations is performed twice, at a pressure of 300 and 150 atm.

The residence time of seawater in the pipeline is temporarily omitted and assumed as the starting value because increasing this parameter will lead to more complexity on BAWL installation. Namely, it will be more feasible to enhance the milling process to obtain smaller grains or change the calcite dosage instead of posing a longer pipeline on the seafloor.

Results are reported in diagram 5.10, which shows that halving the grains

diameters lead to a significant increase in the efficiency, both if we operate with a final pressure of 300 or 150 atm.

Comparing the diagrams (a) and (b) of Figure 5.10, results that the pressure assumes progressively less relevance with the decrease of molar ratio and the increase of grains diameter. In particular, a molar ratio of 0.5 and grains diameter of 5 - 2 μm guarantee the complete reduction of $CaCO_3$ both at 3100 or 1550 m of depth.

In different simulations performed with the same molar ratio, CO_2 reach the same reduction efficiency when calcite is wholly dissolved, despite other parameters. That is explained because imposing the same molar ratio in different simulations involve the dissolution of the same amount of calcite and CO_2 in seawater; therefore, carbon dioxide will react with all bicarbonate ions released by the minerals regardless of other parameters.

Once the effects of the other parameters are evaluated, it is possible to assess the minimum time requirement for mineral dissolution. Until now, the results obtained in diagram 5.10 are performed assuming a time reaction of 100,000 s (about 28 hours), but this value represents the maximum time that the calcite could use to dissolve because it determines the length of the pipeline. Still, calcite dissolution can occur before the discharge point. In many cases, the complete dissolution is obtained before the pipeline end. E.g. if we set the discharge pressure of 150 atm, molar ratio of 0.5, grain diameter of 2 μm and maximum time of 100000 s, calcite will be dissolved entirely at 44,750 s. This considering that in our simulation, the pressure varies linearly with time, so at 44,750 s, the pressure will be around 75 atm: it will set the maximum reaction time at 50,000 seconds (14 hours), complete dissolution of calcite will occur at 40,110 seconds (11.1 hours) at almost 120 atm.

5.5 Working condition comparison - calcite

To find operating points that can ensure complete dissolution of calcite, the functioning of BAWL is simulated with different combinations of pressure, molar ratio and grains size; time and water usage are kept constant. All the parameters values are reported in Table 5.10.

Water usage has not been modified because it has a more negligible effect on calcite dissolution than the other parameters.

Time has not been increased because 100,000 seconds results in a pipeline long about 120 km, a length that is already significant. Moreover, this value is the maximum amount of time that the dissolution can take to complete. If a reaction is completed earlier than 100,000 s, the calcite will be dissolved before the end of the pipeline, which will be consequently re-sized.

Table 5.9: Parameters value that are combined to determine different operating points for calcite application.

Pressure [atm]	300
	150
Molar ratio	1
	0.9
	0.8
	0.7
	0.6
	0.5
	0.4
	0.3
	0.2
	0.1
Grains diameter [μm]	10
	5
	2
Residence time [s]	100,000
T_0 [°C]	16
T_f [°C]	9
Water usage [m^3 tonnes $CO_2{}^{-1}$]	2000

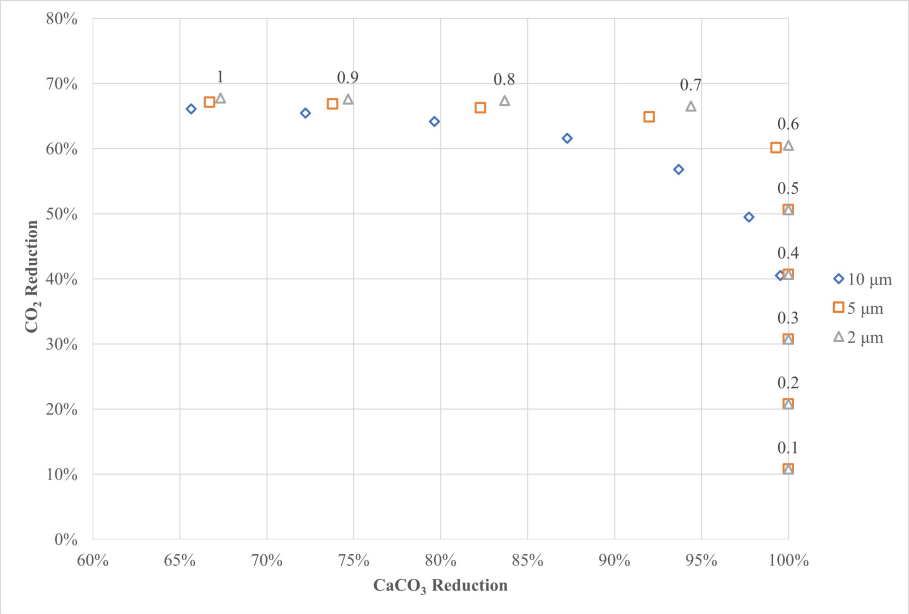

(a) 300 atm

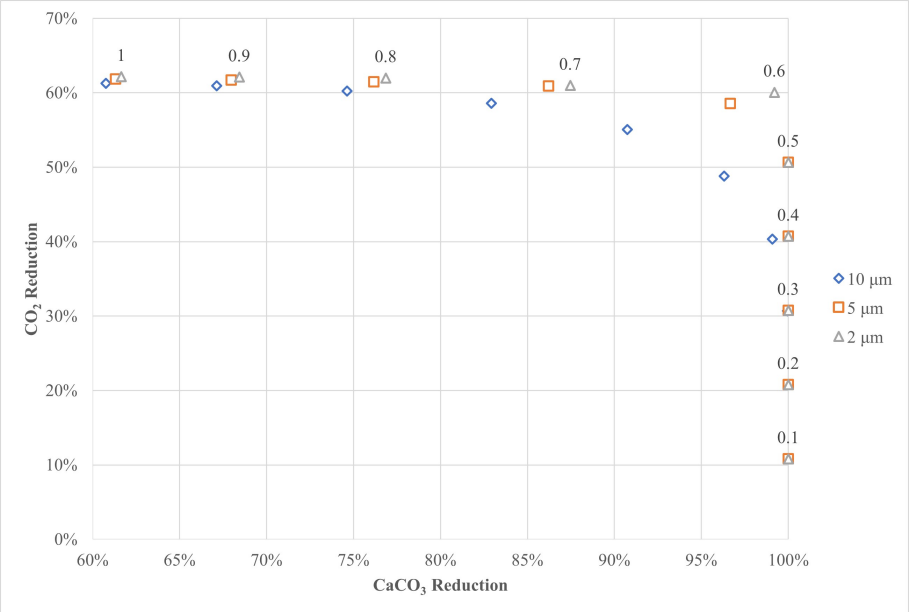

(b) 150 atm

Figure 5.10: Variation of efficiency in calcite and carbon dioxide reduction, in function of different molar ratio and grains diameter. The labels express the molar ratio used, and in each diagram the different series are obtained with different grain diameter reported in the legend. The diagrams (a) and (b) refer respectively to scenario in which we arrive at 300 and 150 atm of depth.

Table 5.10: Parameters value that are combined to determine different operating points for calcite application.

Pressure [atm]	300
	250
	200
	150
	100
	50
Molar ratio	1
	0.9
	0.8
	0.7
	0.6
	0.5
	0.4
	0.3
	0.2
	0.1
Grains diameter [μm]	10
	5
	2
Time [s]	100,000
T_0 [°C]	16
T_f [°C]	9
Water usage [m^3 tonnes $CO_2{}^{-1}$]	2000

The simulation results that give a complete dissolution of calcite are all reported in the Figure 5.11: pressure and calcite's grain diameters are represented on the horizontal axis; the Z-axis represents the efficiency of CO_2 reduction. The point's colours indicate the time in hours required for complete dissolution.

CO_2 reduction gives us different information. It corresponds to the moral ratio used: if calcite is completely dissolved, the $CaCO_3$ will consume all carbon dioxide with which can react; e.g. if the molar ratio of calcite is 0.2, when the mineral is all dissolved, the bicarbonate ions released will react with the 20% of CO_2. Moreover, Z-axis implicitly indicate the amount of calcium hydroxide that will be necessary to neutralize the remaining CO_2: knowing the moles of carbon dioxide remaining, it is possible to calculate the calcium hydroxide needed to neutralize it.

The more favourable operative points are the ones that combine a high reduction of CO_2, low pressure and high grains diameter. From Figure 5.11, it is possible five main operating points that optimize different parameters as described in the list below.

A Combine minimum pressure and maximum CO_2 reduction for 10 μm particles.

B Operates with minimum pressure at medium size grains.

C Returns maximum carbon dioxide reduction with 5 μm diameters grains.

D Achieves maximum carbon dioxide reduction obtainable at 50 atm.

E Gives maximum carbon dioxide reduction.

The operating points are analyzed deeper in chapter 6, where a costs analysis is performed. However, some conclusions can be already deduced.

To achieve a reduction of the 60% of CO_2 injected, the only option is to have a pipeline that conducts at least 250 atmospheres of depth, mill the calcite particles to 2 μm and have a pipeline that allows a residence time of 100,000 seconds (about 27 hours). If the site-specific condition does these conditions, the maximum carbon dioxide reduction will be 50%, and the remaining part should be neutralized with $Ca(OH)_2$.

Grains of 10 μm diameters are not suitable for BAWL: a final CO_2 reduction of 0.2 is not feasible because the 80 % of carbon dioxide would be neutralized with calcium hydroxide. It is important to stress that the 10 μm diameters grains could dissolve totally, but not in a suitable time for our technology.

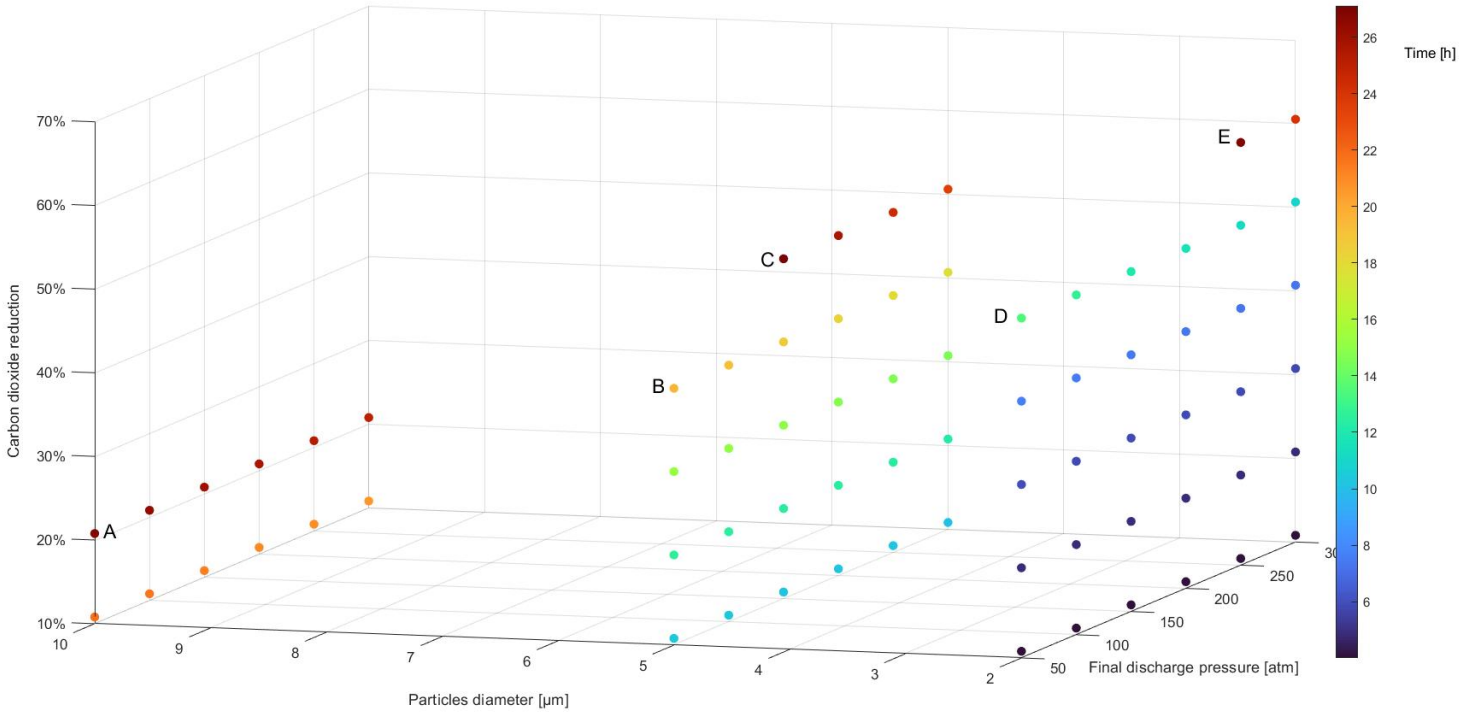

Figure 5.11: Operating points that guarantee a complete dissolution of calcite

5.6 Sensitivity analysis - dolomite

Analyzing dolomite dissolution, we have to keep in mind two main differences between calcite and dolomite: dolomite kinetics is much slower than those of calcite, and the stoichiometric reaction of dolomite and CO_2 has a ratio of $0.5 : 1$ instead of $1 : 1$ (see reaction 3.5). Hereinafter the molar ratio value expresses the proportion to stoichiometric coefficient, e.g. a molar ratio of 0.25 means that dolomite has been dosed as a fourth stoichiometric amount, so 0.125:1.

To find suitable parameters value for dolomite dissolution, it has been applied the same methodology as that used for calcite: starting from the base case "NS" in Table 5.6, we have assigned the same range of value to parameters applied to calcite.

Water usage

In the preliminary sensitivity analysis, the water usage results as the parameters less influential on calcite dissolution for "NS" condition (Table 5.8). So, in this section, it is kept constant at 2000 m^3.

Molar ratio

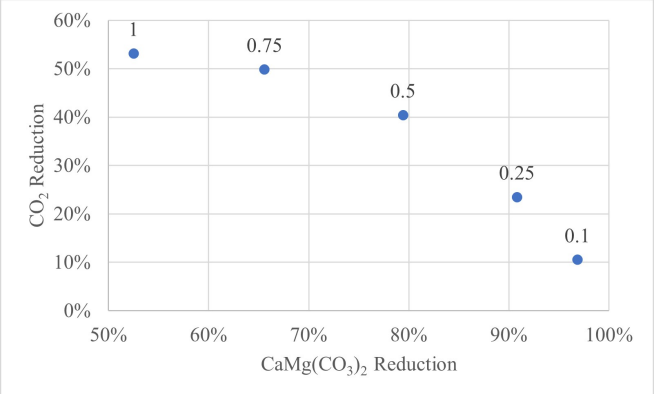

Figure 5.12: Dolomite and carbon dioxide reduction in function of molar ratio.

None of the molar ratio examined allow a complete dissolution of dolomite (Figure 5.12). The decrease of molar ratio enhance the reduction of dolomite and decrease the CO_2 consumption, but its not enough to ensure a complete dissolution of dolomite.

Reaction time

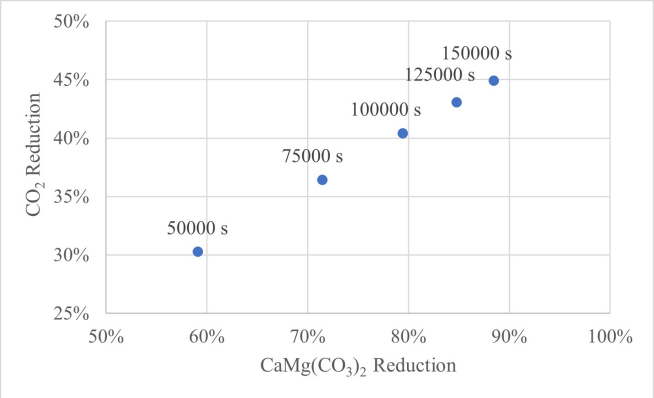

Figure 5.13: Dolomite and carbon dioxide reduction in function of the residence time of the solution in the pipeline.

The increase of the reaction time leads to an increase of the dolomite dissolution and CO_2 reduction (Figure 5.13). Increasing the reaction time until 150,000 seconds (about 42 hours) leads to an improvement of dolomite dissolution to 88%. For calcite, a residence time of 150,000 seconds will lead to a complete dissolution at the same conditions. For dolomite, it will be required to combine the efficiency effect of different parameters to achieve the complete dissolution of the carbonate minerals.

Initial temperature

From sensitivity analysis temperature variation contributes considerably to dolomite dissolution (Table 5.8).

The temperatures considered are the surface temperature that the Mediterranean Sea can assume during the year; the dolomite dissolution can vary from 74.4% to 82.3% (Figure 5.14). Dolomite dissolution is confirmed more influenced by temperature than calcite (Figure 5.6).

Final pressure

Decrease the final discharge pressure that BAWL pipeline reach leads to reducing dolomite and carbon dioxide dissolution (Figure 5.15). As for calcite (Figure 5.7), a high reduction of depth (of 83%) leads to a less pronounced decrease in dolomite dissolution, namely a decrease of the 6% (from 79 to 75%).

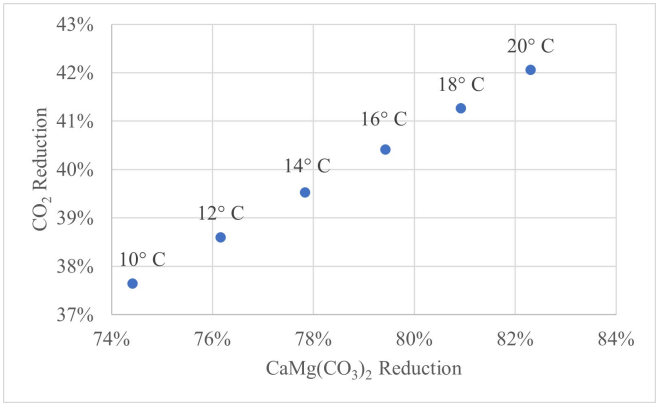

Figure 5.14: Dolomite and carbon dioxide reduction in function of the initial temperature.

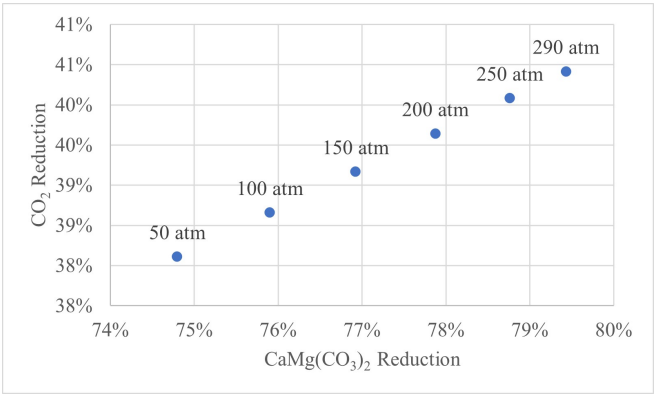

Figure 5.15: Dolomite and carbon dioxide reduction in function of final discharge pressure.

Dolomite dissolution because the dissolution seems substantially slower than the calcite. Even if decrease the depth of discharge from 3000 to 516 meters enhances the feasibility of BAWL considerably, the leak of efficiency could compromise heavily than for calcite the complete dissolution of the minerals. Decrease to 50 atm the discharge point could be made only if other parameters can compensate for this diminishing efficiency.

Grains diameter

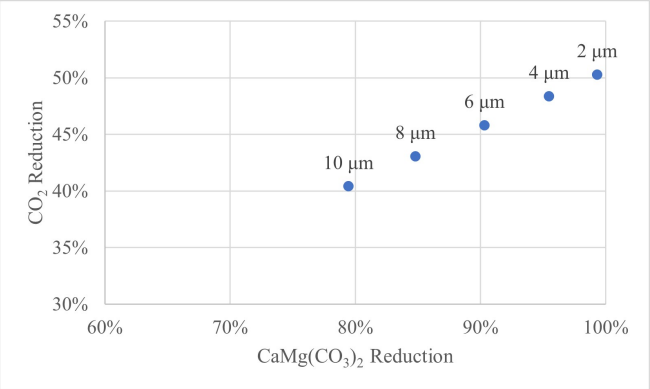

Figure 5.16: Dolomite and carbon dioxide reduction in function of diameters of the grains.

Decrease the diameters of the grains increase the dolomite and CO_2 reduction (Figure 5.16). Among the other parameters investigated, the size of the particles is the one that approaches more on the complete dissolution of dolomite without compromise significantly the efficiency of BAWL (Figure 5.17). The other parameter that allows an almost complete dissolution of dolomite is the molar ratio equal to 0.1, but this reduces the CO_2 consumption to 10%.

The decrease of grains diameter and molar ratio are the man factor that take the dolomite closer to the complete dissolution, which is not reach in these simulations.

Dolomite complete dissolution is therefore more difficult to achieve then that of calcite. This was yet perceivable from Table 5.7: with the same conditions, at discharge point dolomite dissolution will not be progressed as calcite.

The simulation that most approach a complete dolomite dissolution that one that is considered a particles size of 2 μm in Figure 5.16. At that point,

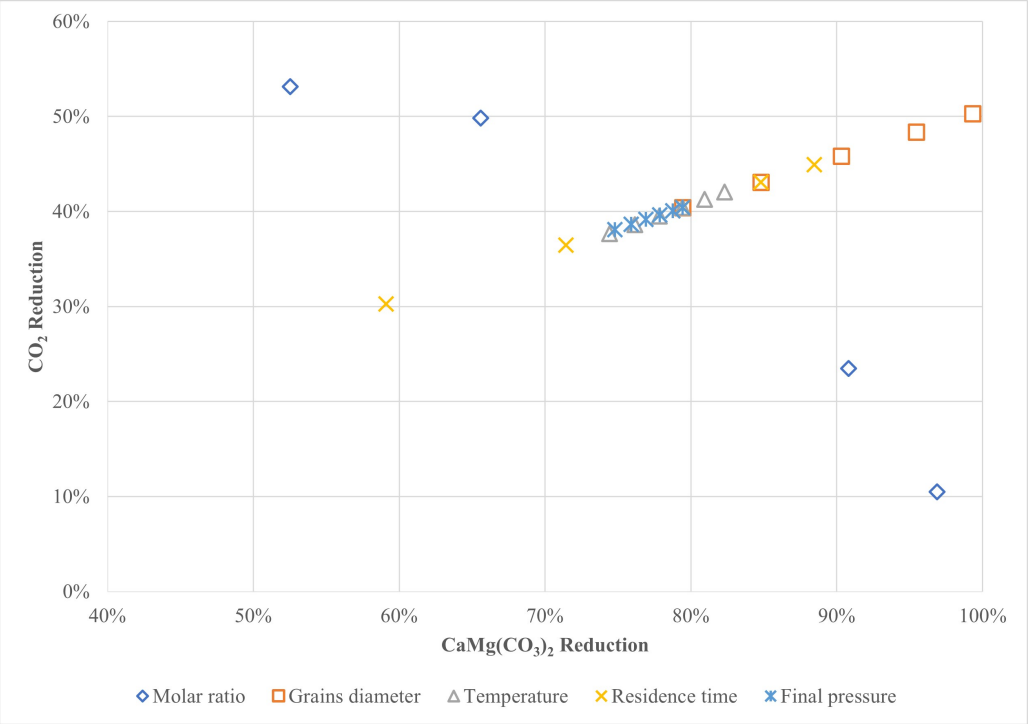

Figure 5.17: Dolomite and carbon dioxide reduction in function of the different parameters.

the SI of dolomite is -0.29, a value that generally allows a complete dissolution of minerals; this means that the main issue to overcome is the time that dolomite will require to dissolve entirely.

From the analysis, it is possible to conclude that to achieve complete dissolution of dolomite, more than one parameter should be varied from the "NS" starting value considered in Table 5.6. While for calcite dissolution, changing individually molar ratio, reaction time and diameter of the grains lead to complete calcite dissolution.

It is crucial to remind that for the functioning of BAWL, the carbonate minerals must be all dissolve before the discharge. Operating points that do not guarantee a complete consumption of the mineral are not acceptable for BAWL.

The analysis of molar ratio and grains diameter can give us results on suitable particles size required to achieve complete dissolution of dolomite in a feasible time.

Figure 5.18 reports the result of simulation which combine different molar ratio and grains diameter; the tests are performed with two sets of pressure: 300 and 50 atmosphere.

We can see that under no circumstance analyzed, the dolomite of 10 μm can dissolve entirely in the given time. Since the 2 μm dolomite completes the dissolution if the molar ratio is 0.4 or lower, bigger grains could potentially dissolve because SI and pH allow it, but the time required will be too high for the BAWL application.

Analyzing the trend of 5 μm, we can see that at 300 atm, the complete dissolution of dolomite is reached only if the molar ratio is equal to or lower than 0.3, so the 70 % of CO_2 should be neutralized with hydroxide. The results are more promising with the grains of 2 μm, because the simulations performed with this measure of grains reach the complete dissolution of dolomite at higher rates. However, it is important to stress that it will be challenging to achieve a complete dissolution using a molar ratio of 0.5; even if the dolomite reduction is about 99.4% at 100,000 s, the reaction time should be increase to 195,464 seconds (54 hours) to achieve complete dissolution.

The results presented until now do not show any benefits of using dolomite instead of calcite. For completeness, we can try to find some feasible points of working for BAWL.

To enhance dissolution, two solutions can be investigated: increase the reaction time, or increase the amount of water used on tonne of CO_2. The increase of these two parameters was excluded until now because of the engineering effort involved or the limited consequent impact on dissolution.

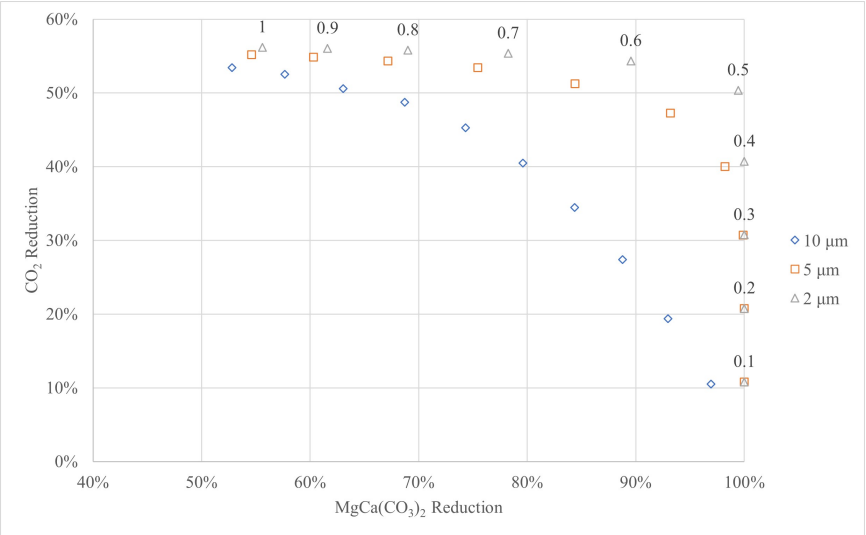

(a) 300 atm

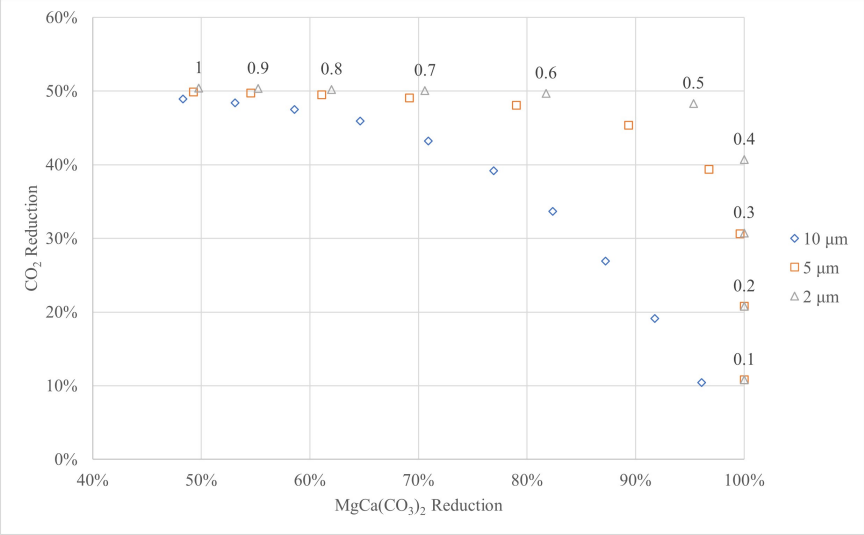

(b) 150 atm

Figure 5.18: Variation of efficiency in dolomite and carbon dioxide reduction, in function of the different molar ratio and grains diameters. The labels express the molar ratio in relation to stoichiometric conditions. In each diagram, the different series are obtained with different grain diameters reported in the legend. Graphs (a) and (b) refer respectively to the scenarios in which we arrive at 300 and 150 atm of depth.

However, to enhance the dolomite dissolution, it could be necessary.

As a first assessment, the amount of water and maximum time of the reaction are increased to 2500 m^3 and 150,000 seconds (42 hours), respectively. Results are reported in diagram 5.19 where are compared to the base case of 2000 m^3 and 100,000 seconds (28 hours). All these simulations are performed with a particles size of 2 μm to enhance the dissolution.

Figure 5.19a shows that the simulations performed with a molar ratio of 0.5 and a final depth of 300 atm achieve the complete dissolution of dolomite. In the other cases, the dolomite reduction is still increased but not to 100%.

It is essential to highlight that in Figure 5.19(b), the point with a molar ratio of 0.5 and a final depth of 300 atm do not reach the complete dissolution of dolomite, but the 99.4%. Increasing reaction time to 150,000 seconds, still the dissolution will not be completed.

Increase reaction time, and water volume seems to be the only option to achieve complete dissolution of dolomite and a CO_2 reduction of at least the 50%.

5.7 Working condition comparison - dolomite

As done for calcite, the operating points that ensure complete dissolution of dolomite are found by combining different values of parameters reported in Table 5.11. The grains size considered are only 2 μm, whereas water usage has been considered from 1500 to 2500 m^3.

The points that ensure complete dissolution of dolomite are reported in diagram 5.20: the horizontal axis represent the water consumption and final pressure of discharge, while the Z-axis report the percentage of CO_2 reduction achieved. Points colour indicate the time that dolomite takes to dissolve.

The most favourable operation points are the ones that maximize CO_2 reduction and minimize depth of discharge, time requirement and water consumption.

F Return the maximum CO_2 reduction with a consumption of water of 1500 $m^3\,CO_2\,tonne^{-1}$.

G Works at the minimum pressure and water usage.

H Gives the maximum carbon dioxide removal at 50 atm.

I Achieve maximum carbon dioxide reduction.

To obtain a dissolution of 50%, the minimum volume of water we should use is 2500 m^3, and the pipeline should arrive at least 250 atm of depth

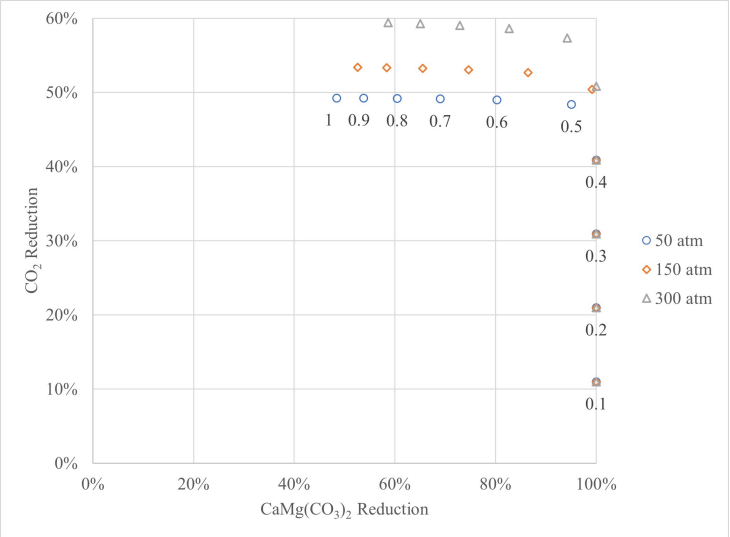

(a) 2500 m^3 and 150,000 s

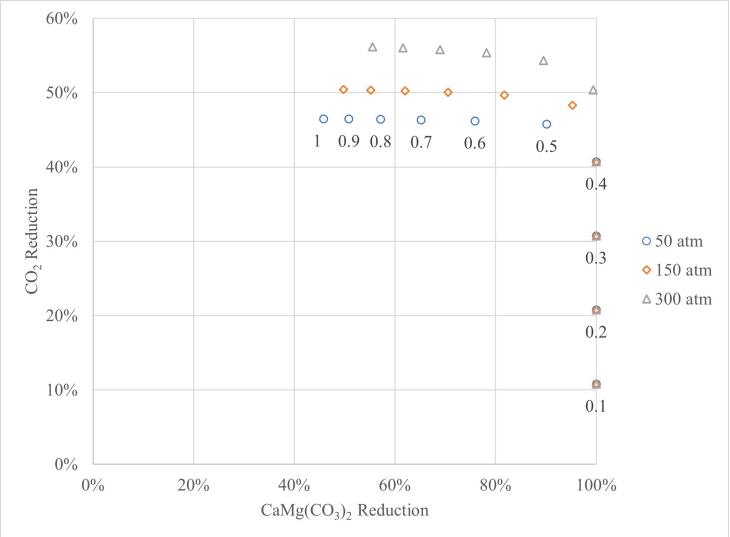

(b) 2000 m^3 and 100,000 s

Figure 5.19: Variation of efficiency in dolomite and carbon dioxide reduction in function of different residence time and water consumption. The label express the molar ratio in relation to the stoichiometric condition. In each diagram the different series refer to the discharge depth reported in the legend. Volume of water used to dissolve 1 tonne of CO_2 and the time used are reported in the figure caption.

(2582.5 m). If a CO_2 reduction of the 40% is acceptable, the pressure could be reduced until 50 atm (516.5 m).

Table 5.11: Parameters value that are combined to determine different operating points for dolomite application.

Pressure [atm]	300 250 200 150 100 50
Molar ratio	1 0.9 0.8 0.7 0.6 0.5 0.4 0.3 0.2 0.1
Grains diameter [μm]	2
Time [s]	150,000
T_0 [°C]	16
T_f [°C]	9
Water usage [m^3 tonnes $CO_2{}^{-1}$]	2500 2000 1500

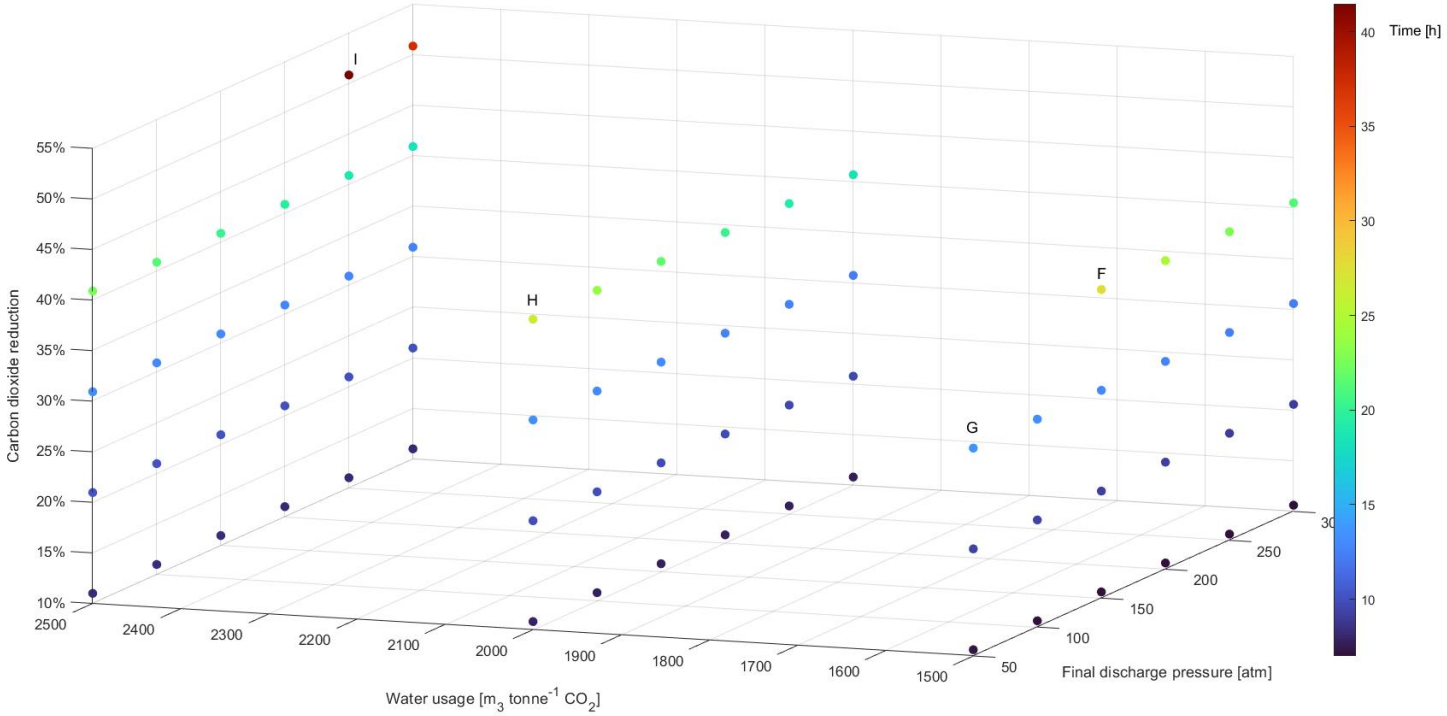

Figure 5.20: Operating points that guarantee a complete dissolution of dolomite.

Chapter 6

Case studies

From Figures 5.11 and 5.20, nine operational points, that optimize different combination of parameters, are identified. This chapter illustrates a preliminary costs analysis on these points to evaluate the working condition that could be preferred.

6.1 Calcite case studies

The five operational points selected for calcite implementation, from the case A to E, are presented in Table 6.1. Before proceeding with the costs analysis, the points are analyzed deeper to re-calculate the minimum time for dissolution. In the simulations reported in diagram 5.11, the pipeline is long 120 km to ensures a residence time of 100,000 seconds. However, if dissolution is complete in less time, there is no reason why the pipeline should be as long.

In Figure 5.11, there are reported indications about the time required for the complete calcite dissolution but is just assessment. Because in the simulations, pressure and temperature change linearly with time, and in a shorter pipeline, the value of pressure and temperature will evolve faster, changing the reaction time. Therefore, for the five case studies, the minimum time required for the reaction and pipeline length are re-calculated.

Table 6.2 reports the time and length assumed for preliminary calculations performed in chapter 5, and the new values re-calculated for base case analysis. The differences between the residence time and the time at which the calcite effectively is dissolved are reduced. However, the pipeline length is fixed at the rounded value at which the dissolution is completed, e.g. in case study B, a residence time of 72,000 seconds does not ensure complete dissolution of calcite. The length variation is calculated between the 120 km

Table 6.1: Parameters of calcite case studies

	A	B	C	D	E
Water usage [$m^3\,tonne^{-1}\,CO_2$]	2000	2000	2000	2000	2000
Molar ratio	0.2	0.4	0.5	0.5	0.6
Grains diameter [μm]	10	5	5	2	2
Final discharge Pressure [atm]	50	50	150	50	250
Final discharge depth [m]	517	517	1550	517	2583
Residence time [s]	97,000	73,000	98,000	47,000	93,000
Pipeline length [km]	116	88	118	56	111
Initial temperature [°C]	16.0	16.0	16.0	16.0	16.0
Final temperature [°C]	9.0	9.0	9.0	9.0	9.0
pH	6.02	6.33	6.45	6.48	6.56
CO_2 Reduction	20.8%	40.7%	50.6%	50.6%	60.5%
SI $CaCO_3$	-1.07	-0.51	-0.30	-0.20	-0.15
SI $CaMg(CO_3)_2$	-1.38	-0.23	0.06	0.26	0.35
$Ca(OH)_2$ Usage [$kg\,tonn^{-1}\,CO_2$]	673	504	420	420	335
Total CO_2 stored [$tonn\,CO_2\,y^{-1}$]	172,488	172,488	172,488	172,488	172,488
CO_2 By calcination [$tonn\,CO_2\,y^{-1}$]	116,115	86,944	72,375	72,379	57,853
Net CO_2 stored [$tonn\,CO_2\,y^{-1}$]	56,333	85,543	100,112	100,108	114,635
CO_2 Penalty	67%	50%	42%	42%	34%

previously considered and that resulting from new simulations.

The hydroxide consumption is assessed by knowing how much $Ca(OH)_2$ is required to neutralize the remaining CO_2. Starting from the equation 3.9, the stoichiometric molar ratio between calcium hydroxide and carbon dioxide is 1:2, but in seawater, the reaction is reduced to 1:1.8 (Caserini et al. 2021).

The production of $Ca(OH)_2$ involve the emission of CO_2, namely for each mole of calcium hydroxide produced a mole of CO_2 is produced (see reactions 3.8 and 3.7). Table 6.1 reports the annual tonnes of carbon dioxide emitted to produce the calcium hydroxide for each case study. This amount of carbon dioxide is stored directly in the BAWL plant, where it is produced. This storage reduces the total capacity of BAWL plant because part of the total amount of CO_2 stored comes from the calcination process and not from external sources. The CO_2 penalty express how much of the total annual capacity of the plant is used to store the CO_2 produced for $Ca(OH)_2$ production.

Observing the data of Table 6.1 it is possible to formulate some preliminary remarks, that should be verified with the costs analysis.

Among these points, case A could be less favourable because the consumption of calcium hydroxide is very high: this will influence at the same

Table 6.2: Comparison of pipelines lengths of calcite base cases. The table reports the time and length assumed for preliminary calculations performed in chapter 5, and the new length assessed for case studies analysis.

	A	B	C	D	E
Residence time, Figure 5.11 [s]	100,000	100,000	100,000	100,000	100,000
Dissolution time, Figure 5.11 [s]	95,928	70,596	97,584	48,328	96,612
Residence time, re-calculated [s]	97,000	73,000	98,000	47,000	93,000
Dissolution time, re-calculated [s]	96,520	71,916	97,348	46,376	92,136
Pipeline length, Figure 5.11 [km]	120	120	120	120	120
Pipeline length, re-calculated [km]	116	88	118	56	112
Length variation	-3.1%	-37.0%	-2.0%	-112.8%	-7.5%

time the consumption of electricity and emission of CO_2 resulting from calcination.

If the milling process necessary to obtain grains of 2 μm will not be too expensive compared to 10 and 5 μm grinding, one of the cases D and E will be the most efficient in terms of emissions and costs. Namely, D guarantees a short and superficial pipeline, while E the higher CO_2 reduction and so the lower $Ca(OH)_2$ requirement.

6.1.1 Preliminary cost analysis

Figure 2.2 reports a general diagram of BAWL that illustrates the main costs items related to technology.

Capital and operational costs (CAPEX and OPEX) are assessed for each item described below; Tables 6.3 and 6.4 report the coefficients used in the calculation. The work of Cappello et al. (2021) has assessed the costs of BAWL by machinery producers and literature; these costs assessment is applied to the different case studies analyzed in the thesis.

CAPEX costs are calculated by the price of the device requirement (Table 6.3), and then normalised on the amount of carbon dioxide from external sources that the BAWL can store. Namely, the BAWL plant is characterised by a total storage capacity based on the flow that the pipeline can channel, which in this analysis is fixed, and the quantity of seawater needed for a tonne of CO_2, e.g. 2000 m^3 in calcite application. A portion of this capacity is used to store the CO_2 that is produced for the calcination process. The difference between the total annual capacity of the BAWL plant and the total CO_2 produced annually for calcium hydroxide production gives the net storage capacity of BAWL plant. The CAPEX expense is then amortised on

the equipment's service life, which is assessed to 20 years for each device and 100 years for the pipeline.

BAWL plant is supposed to work without fossil fuel consumption, so the electricity required is produced by renewable resources. The price of electricity considered is 31 €· MWh^{-1}, an assessment of the price of current levelized cost of utility-scale electricity produced by photovoltaic and wind resources (Lyman and Fleming 1940).

Most of the OPEX costs in Table 6.4 are yet normalized on the amount of carbon dioxide stored. The others are normalized on the amount of calcite and hydroxide required for each tonne stored, dates obtainable by table 6.1.

Once that OPEX and CAPEX costs related to each BAWL component are calculated, their sum gives the costs of each case study, expressed as euro on tonne of CO_2 stored.

A summary of which costs derive from the different components of BAWL is here reported.

Calcite supply The calcite price has been calculated considering capital and operating costs of a calcite quarry, and then the transport of minerals for 20 km until BAWL plant.

In the plant scheme $Ca(OH)_2$ is produced on-site, so calcite should be supplied both for the reaction with CO_2 in the pipeline and also for $Ca(OH)_2$ production, whose as approximation requires one mole of calcite for one mole of calcium hydroxide.

Compressor The compressor is necessary to increase the gaseous phase pressure, which makes it possible to dissolve CO_2 in seawater. To assess the energy requirement of compressor, it is necessary to hypothesize the composition of CO_2 flux. The flue gas assumed derives by Steam Methane Reformer for hydrogen production, that is composed in volume by 21% of CO_2, 6% of O_2 and 73% of N_2.

Thanks to the volume and pressure of the flux we can have an esteem of the electricity consumption that is required to obtain the gaseous phase pressure that will allow to dissolve 1 tonne of CO_2 in 2000 m^3 of seawater.

MIX Mixer is the reactor where carbon dioxide, seawater and calcite are mixed. Namely seawater enters trough the top and flow counter-current to the gaseous phase (whose is leaving the compressor) that is injected at the bottom of reactor. In the lower part of the MIX is supplied calcite, so the solution of seawater, CO_2 and minerals flow in the main pipeline.

The only cost considered for the MIX is CAPEX due to the purchase and installation of the reactor, all energy costs related to functioning are allocated on the pumping system.

Milling The milling process is required to grind calcite, which is needed to neutralize CO_2 in the main pipeline but also to produce the calcium hydroxide. For these two processes, the particles size required are different: for the first purpose, we analyze grains sizes of 10, 5 and 2 μm, whereas, for the calciner, calcite particles could be 75 μm.

To obtain different grinding degrees, the type and number of machinery change. A milling machine producer has provided the information to determine the number of machines required and specific electricity consumption related to obtaining a grain's specific dimension.

Generally, different steps are required to obtain a specific grain size. Firstly the stones should be reduced to 25 mm grains. Then the process is differentiated for each size: 70 and 10 μm grains can be milled with the same machines operating at diverse working conditions (with different energy requirements), the particles of 2 μm should be milled with two different machines.

For 5 μm particles, specific indications are not provided, so the CAPEX is assumed the same as the machinery for 2 μm particles. The specific electric consumption changes for each particle size obtained, so it is hypothesized as a mean of 10 and 2 μm energy requirement.

Electric calciner It is the machinery where calcium carbonate $CaCO_3$ is transformed into calcium oxide CaO. This process is endothermic, and an electric process will supply the heat necessary to avoid fossil fuel use.

Slacker In the slacker, CaO reacts with water and forms the calcium hydroxide. This process is exothermic, so no energy requirement is considered; actually, the heat produced in the slacker is recirculated in the electric calciner.

Dissolution Reaction - DR The pipeline can be made of an HDPE tube, with an internal and external diameter of 3500 and 3671 mm, respectively. Knowing tube measures and HDPE density (941 kg $\cdot$ m^{-3}), it is possible to calculate the HDPE requirement at km of pipeline. Moreover, the pipeline would require some ballast, namely concrete blocks.

The esteem of costs associated with the pipeline installation is performed by considering purchased and related costs (fuel, worker and maintenance)

of the necessary ships.

To consider other industrial costs, the final expense of each pipeline is increase by 25%.

All the costs relative to the pipeline are normalized on the kilometers of pipeline to evaluate the installation of different length pipelines that characterize the case study.

Slacked Lime pipeline - SL The secondary pipeline will be made with the same features of DR, but the tube will have an internal diameter of 560 mm. This difference will influence the costs related to HDPE and ballast requirements.

The installation costs are taken into account once for MP and SP.

Pumping system Two main pumps are explicitly considered for handling seawater. The first supplies water to MIX, so it moves water that will flow in the DR. While the other provides the water for the slacked lime pipeline. CAPEX and OPEX will be different because they depend on the amount of seawater that can flow in each pipeline.

In the DR and SL can flow 41563 and 1064 $m^3\,h^{-1}$ respectively. These data are calculated by knowing the section area of each pipeline and the minimum velocity required to avoid sedimentation in the pipeline (1.2 ms^{-1}).

Other costs The final cost is increased by 10%, to consider other costs like maintenance, workers. A interest rate is not considered in this analysis.

6.1.2 Preliminary cost analysis results - calcite

Table 6.5 report the resulting costs for each case study.

The main CAPEX costs are related to pipeline installation, while the other machinery has a limited impact on the total costs (from 4% to 5% in the different cases).

OPEX costs are mainly due to the electricity requirement: summing all the BAWL plant's electric consumption, the results go from 42% to 58% of the total costs depending on the different cases.

In the different case studies, calcite supply influence the costs of 7%-13%.

Figure 6.1 reports as label the different percentages for each case study. Focusing on the cheapest case studies E and D, we see that D has a pipeline longer, about half of the pipeline E. This difference compensates for the calcium hydroxide saving of E. Further study on CO_2 emission should assess if this compensation is valid also for emissions. However, the high reduction

Table 6.3: CAPEX costs (Cappello et al. 2021)

DR	Installation	95,750	€· km^{-1}
	HDPE supply	861,000	€· km^{-1}
	Pipeline production	646	kWh · km^{-1}
	Ballast	76,000	€· km^{-1}
SL	HDPE supply	96,430	€· km^{-1}
	Pipeline production	72	kWh · km^{-1}
	Ballast	228,000	€· km^{-1}
Milling process	2 μm	2,907,681	€
	5 μm	2,907,681	€
	10 μm	1,204,602	€
	70 μm	1,204,602	€
MIX		434,000	€
Pumping system	DR	608,000	€
	SL	25,000	€
Compressor		433,200	€
Calciner		101,650	€· $Ca(COH)_2$ tonne $^{-1}$ · h^{-1}
Slacker		41,300	€· $Ca(COH)_2$ tonne $^{-1}$ · h^{-1}
Electricity price		0.031	€· kWh $^{-1}$

Table 6.4: OPEX costs (Cappello et al. 2021)

Milling process	2 μm	247	kWh · Mineral tonne $^{-1}$
	5 μm	190	kWh · Mineral tonne $^{-1}$
	10 μm	133	kWh · Mineral tonne $^{-1}$
	70 μm	28	kWh · $Ca(OH)_2$ tonne $^{-1}$
Pumping system	DR	237	kWh · CO_2 tonne $^{-1}$
	SP	15	kWh · CO_2 tonne $^{-1}$
Compressor		141	kWh · CO_2 tonne $^{-1}$
Calciner		1.126	€· CO_2 tonne $^{-1}$
Electricity price		0.031	€· kWh^{-1}

of depth that we achieve with D and the consequent BAWL variation of feasibility and impact on sea could be worthy of efficiency loss.

Case study D turn out the most efficient point of applying the BAWL technology because the faster dissolution of case study D involves a shorter pipeline, an advantage on the costs and feasibility of the technology.

Table 6.5: Calcite case studies costs, all item expressed as €· CO_2 tonne $^{-1}$ from external source.

		A	B	C	D	E
CAPEX	DR and SL pipeline	34	17	19	9	16
	Milling		2	2	2	2
	Calciner and slacker	0.6	0.4	0.4	0.4	0.4
	MIX, compressor, pump	1.3	0.9	0.7	0.7	0.7
	Total CAPEX	38	20	22	12	19
OPEX	Calcite supply	7	8	8	8	9
	Calcite milling	2	6	6	9	11
	Calciner	24	18	15	15	12
	Compressor, pump	12	12	12	12	12
	Total OPEX	45	44	41	44	44
Other costs (10%)		8	6	6	6	6
Total		91	71	70	62	68

6.2 Dolomite case studies

Similarly as done for calcite application on BAWL, the case studies from F to I identified from Figure 5.20 are investigated deeper, to determine precisely the length of the pipeline and the calcium hydroxide requirement (Tables 6.6).

Comparing with calcite case studies, the average pipeline length and calcium hydroxide requirement increase with the use of dolomite (Tables 6.1 and 6.6).

Among the dolomite case studies, F is characterized by high efficiency in carbon dioxide storage because it considers the use of only 1500 m^3 CO_2 $tonne^{-1}$ and it guarantees the 40% of CO_2 reduction. Of the total CO_2 that the plant can store annually, 59% is produced for the $Ca(OH)_2$ production as for case H, which stores less CO_2 annually.

Comparing calcite and dolomite operating points, the high $Ca(OH)_2$ requirement and the increase in water usage reduces the quantity of external CO_2 that the BAWL plant can store (except the case A and B).

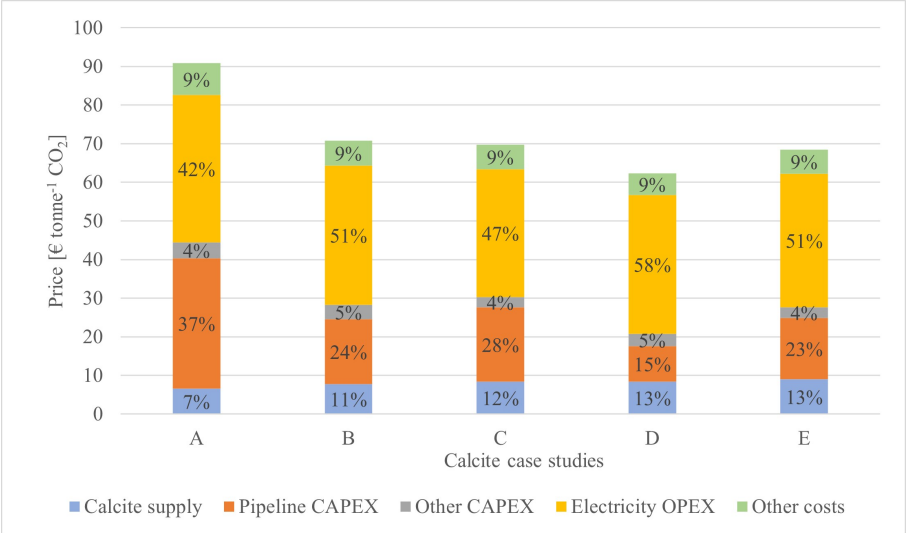

Figure 6.1: Cost contribution in the calcite case studies.

6.2.1 Preliminary cost analysis results - dolomite

The costs items utilized for calcite application on BAWL are valid also for dolomite, but some differences should be highlighted:

- Dolomite supply should be add to costs list. But calcite supply can not be totally eliminated from the costs, because it is still needed to produce calcium hydroxide. As first approximation we can use same costs for calcite and dolomite supply.

- The variation of the water usage on CO_2 tonne will influence the energy requirement of the compressor because a different amount of CO_2 will de dissolved in the same amount of seawater. The pumping system functioning will not change because the volume of water pumped depends on the pipeline flow, which remains constant. As a first approximation, the OPEX of the compressor can be kept constant.

The calculated costs are reported in Table 6.7. The cheapest working point corresponds to case G.

Comparing the calcite and dolomite most favourable operative points, respectively D and G, the calcite application on BAWL results less expensive and characterized by a higher storage capacity and more feasibility, in terms of pipeline length and dept.

The costs distribution for dolomite application follows the same division as that of calcite. Namely, the higher costs are allocated on electricity OPEX

Table 6.6: Parameters of dolomite case studies

	F	G	H	I
Water usage $[m^3 CO_2 tonne^{-1}]$	1500	1500	2000	2500
Molar ratio	0.4	0.3	0.4	0.5
Grains diameter [μm]	2	2	2	2
Final discharge Pressure [atm]	150	50	50	250
Final discharge depth [m]	1550	517	517	2583
Initial temperature [°C]	16.0	16.0	16.0	16.0
Final temperature [°C]	9.0	9.0	9.0	9.0
Pipeline length [km]	120	72	120	180
Residence time [s]	100,000	60,000	100,000	150,000
pH	6.27	6.16	6.35	6.42
CO_2 Reduction	40.5%	30.6%	40.7%	50.8%
SI $CaCO_3$	-0.54	-0.73	-0.53	-0.56
SI $CaMg(CO_3)_2$	-0.32	-0.67	-0.29	-0.32
$Ca(OH)_2$ Usage [$kg\,tonn^{-1}$ CO_2]	595	695	593	492
Total CO_2 stored [$tonn\,CO_2\,y^{-1}$]	229,983	229,983	172,488	137,990
CO_2 By calcination [$tonn\,CO_2\,y^{-1}$]	136,801	159,712	102,286	6,7860
Net CO_2 stored [$tonn\,CO_2\,y^{-1}$]	93,182	70,271	70,201	70,130
CO_2 Penalty	59%	69%	59%	49%

(38% to 56% in the different cases) and the pipeline production and installation (from 22% to 42%). However, in the case of study E, the pipeline costs are higher than those of electricity (Figure 6.2). Therefore, are these the sector where more interest should be paid.

Analyzing the water consumption, it is possible to conclude that consuming less seawater on CO_2 stored enhanced the capacity of BAWL system: the case F is the ones that can store more CO_2 among dolomite operative points (Table 6.6). The seawater utilizes in the plant is always the same because it depends on the pipeline system. At the same time, the capacity of storage is determined by the quantity of CO_2 dissolve in the same volume of water.

However, case H achieve the same CO_2 reduction with a less deep pipeline. So, if the application site does not allow to discharge the solution at 150 atm, the parameter of case H should be followed.

Table 6.7: Dolomite case studies costs, all item expressed as €· CO_2 tonne $^{-1}$ from external source.

		F	G	H	I
CAPEX	DR and SL pipeline	21	17	28	42
	Milling	2	3	3	3
	Calciner and slacker	0.5	0.6	0.5	0.4
	MIX, compressor, pump	0.8	1.1	1.1	1.1
	Total CAPEX	24	21	32	46
OPEX	Calcite supply	8	8	8	7
	Calcite milling	7	5	7	8
	Calciner	21	24	21	17
	Compressor, pump	25	12	12	12
	Total OPEX	61	49	48	45
Other costs (10%)		9	7	8	9
Total		94	78	88	100

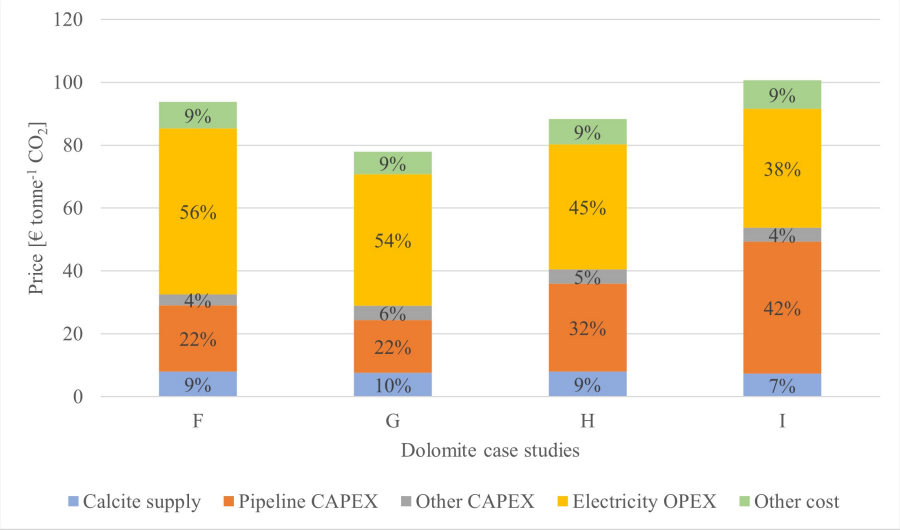

Figure 6.2: Cost contribution in different dolomite case studies.

Chapter 7

Conclusions

In this thesis are performed different rate implementation within PHREEQC software, which has allowed to perform analysis on carbonate minerals dissolution applied to a technology of CO_2 storage. Namely, different feasible operative points of the application of BAWL are determined both for calcite and dolomite usage.

Comparing dolomite and calcite operative points, the use of $CaCO_3$ is the most advantageous for the application of BAWL (Table 6.1 and 6.6). $MgCa(CO_3)_2$ usage is feasible, but BAWL functioning will be less efficient, more expensive and impacting.

Other carbonate minerals could be considered to substitute calcite, but those characterized by high magnesium quantitative in the crystal lattice (magnesite) are described by slower dissolution rate than calcite (L. Chou, Garrels, and Wollast 1989). Therefore they will face the same dolomite problems. Aragonite could be an excellent alternative to calcite because they have the same chemical composition and similar kinetics (L. Chou, Garrels, and Wollast 1989).

In nature, calcite crystal lattice could present impurities of other minerals (e.g. aragonite and dolomite); nevertheless, this should not be a problem because the dissolution rate constants are extrapolated by tests performed on natural calcite samples that naturally have small impurities of magnesium (Palandri and Kharaka 2004). Therefore, the presence of such traces should not compromise calcite dissolution. However, it is essential to notice that in the case studies C, D and E, the most efficient BAWL working point, the Saturation Index on dolomite, is higher than 0, and significant presence of magnesium in the calcite lattice could slow down the mineral dissolution. At the same time, phenomenons of precipitation will not occur because, in seawater, the mineral precipitate at saturation states Ω higher than $20 - 25$ (SI = 1.3 - 1.4) (Pytkowicz 1973).

The ranges of values of the parameters evaluated suitable for BAWL working are here reported. All these considerations refer to calcite application.

- Molar ratio between calcite and CO_2: the maximum dosage of mineral resulted as 60% of the stoichiometric dose, but this value is acceptable only if other parameters as pipeline dimension are maximized. A molar ratio of 0.5 implies a 10% efficiency loss, but it makes BAWL more applicable.

- Consumption of water: it is assessed as 2000 m^3 of seawater on a tonne of CO_2 stored, at which we should sum the water requirement for hydroxide dissolution, fixed at 150 $m^3\,CO_2\,tonne^{-1}$.

- Diameters of minerals particles: the most convenient grains size is about 2 μm, because it speeds up calcite dissolution, allowing a shorter pipeline. Its lower costs compensate for the higher costs related to CAPEX and OPEX costs of the milling process.

- Length of the pipeline: 56 km is the minimum length that the pipeline should assume to guarantee a residence time of about 46,500 seconds (13 hours). Nevertheless, a longer pipeline could be required to achieve a higher CO_2 reduction, but the longest pipeline considered is about 117 km (Table 6.1).

- Depth of the pipeline: minimum pressure that we have considered is 50 atm (about 517 meters of depth). Higher pressure can be achieved for more significant CO_2 reduction, but lower depths are preferable for environmental impact, BAWL feasibility and discharge control.

Focusing on the depth of the pipeline, the pressure enhances the dissolution of carbonate minerals and consequently reduces the requirement of calcium hydroxide to neutralize the remaining CO_2. Indeed, in Table 6.1 it is possible to see that the dosage of carbonate with a molar ratio of 0.6, and achieve a CO_2 reduction of the 60% is feasible only reaching at least the 2583 meters of depth (250 atm). Discharge the solution at 50 atm is possible only if the reduction of carbon dioxide operated by the calcite is reduced at 50%, and the other 50% will be reduced thanks to the calcium hydroxide.

It is crucial to highlight that discharge the solutions at lower depths can impact ocean acidification, a phenomenon that involves the surface layers of the ocean. Namely, the solution released by BAWL contains bicarbonate ions (HCO_3^-), which can enhance the sea buffer capacity.

The BAWL technology enhances two main aspects of the original AWL configuration (Rau and Caldeira 1999). It increases the storage lasting,

thanks to the slurry injection at high depth and the use of calcium hydroxide, that not allow CO_2 degassing. Moreover, it reduces the consumption of water from 7000 to 2000 m^3 on CO_2 tonne.

Buffered Accelerated Weathering of Limestone can be applied to retrofit existing industrial plants for limiting or avoiding its CO_2 emissions. Other feasible applications combine BAWL with bio-energy or blue hydrogen production to be used both for negative emissions implementation (BECCS) or zero-emission technology. Blue hydrogen is produced by a steam methane reformed process, which CO_2 emissions are not released in the atmosphere but captured and stored.

BAWL is a modular technology because the CO_2 storage capacity changes depending on the number of pipelines installed. The scheme 2.2 represent a single module, but increasing the number of pipelines and the capacity of others BAWL components, the tonnes of carbon dioxide that the plant can store increase. The minimum capacity of storage changes depending on the working conditions of BAWL, but it go from 56 kt/y to 114 kt/y (Tables 6.1 and 6.6).

The storage system is more convenient if the CO_2 emitter is in the proximity of the sea so that the BAWL can be installed directly at the carbon dioxide source. The industrial plant costs and emissions are significantly reduced if a calcite quarry is easily available. A high distance will increase costs and emissions related to transport.

The preliminary costs analysis, performed on calcite case studies, assessed the price of storing one tonne of CO_2 in a range of 62-92 €· CO_2 tonne $^{-1}$. These prices consider the CO_2 from external sources, net of the carbon dioxide produced at the plant for the calcium hydroxide requirement. The production of calcium hydroxide reduces the efficiency of CO_2 storage and affect the costs; however, the most convenient case study (case D) is not that characterized by higher efficiency (case E). Therefore, it can be convenient for BAWL applications to work in less efficient conditions if they allow a more feasible plant.

Further study should examine in depth:

- BAWL impacts on ecosystem present at different depths in the ocean, to understand if the increase of alkalinity could be dangerous for some of the marine species that we find at different depths.
- The impurities in carbonate minerals or calcium hydroxide, which could be toxic to the marine environment and prevent the complete dissolution of carbonate minerals.

- The dissolution kinetics of calcium hydroxide and its interaction with the solution of seawater - CO_2 - calcite.
- A Life-cycle assessment of the technology to assess the overall impact of BAWL. Furthermore, it will evaluate the actual capacity of CO_2 storage, net of all the emissions correlated to the technology working and installation.

The thesis has confirmed the feasibility of storing the CO_2 as bicarbonate in the ocean, with a preliminary costs that can vary from 60 to 100 Euro CO_2 tonne from external sources.

Bibliography

Appelo, C Anthony J and Dieke Postma (2004). *Geochemistry, groundwater and pollution*. CRC press.

Appelo, CAJ (2015). "Principles, caveats and improvements in databases for calculating hydrogeochemical reactions in saline waters from 0 to 200°C and 1 to 1000 atm". In: *Applied Geochemistry* 55, pp. 62–71.

Appelo, CAJ, HE Beekman, and AWA Oosterbaan (1984). "Hydrochemistry of springs from dolomite reefs in the southern Alps of northern Italy". In: *IAHS Pub* 150, pp. 125–138.

Appelo, CAJ, E Verweij, and H Schäfer (1998). "A hydrogeochemical transport model for an oxidation experiment with pyrite/calcite/exchangers/organic matter containing sand". In: *Applied geochemistry* 13.2, pp. 257–268.

Archer, David (2005). "Fate of fossil fuel CO_2 in geologic time". In: *Journal of Geophysical Research: Oceans* 110.C9.

Bui, Mai et al. (2018). "Carbon capture and storage (CCS): the way forward". In: *Energy & Environmental Science* 11.5, pp. 1062–1176.

Busenberg, Eurybiades and Niel Plummer (1982). "The kinetics of dissolution of dolomite in CO_2-H_2O systems at 1.5 to 65°C and 0 to 1 atm PCO_2." In: *American Journal of Science* 282.1, pp. 45–78.

Cappello, G et al. (2021). "Buffered accelerated weathering of limestone for storign CO_2: material and energy balance". In preparation.

Caserini, S et al. (2021). "Buffered accelerated weathering of limestone for storing CO_2: chemical background". Submitted to International Journal of Greenhouse Gas Control.

Chou, LEI, Robert M Garrels, and Roland Wollast (1989). "Comparative study of the kinetics and mechanisms of dissolution of carbonate minerals". In: *Chemical geology* 78.3-4, pp. 269–282.

Chou, Wen Chen et al. (2015). "Potential impacts of effluent from accelerated weathering of limestone on seawater carbon chemistry: A case study for the Hoping power plant in northeastern Taiwan". In: *Marine Chemistry* 168, pp. 27–36.

Coninck, H de et al. (2018). "Strengthening and implementing the global response". In: *Global Warming of 1.5°C. An IPCC Special Report on the impacts of global warming of 1.5°C above pre-industrial levels and related global greenhouse gas emission pathways, in the context of strengthening the global response to the threat of climate change, sustainable development, and efforts to eradicate poverty*. Intergovernmental Panel on Climate Change (IPCC), pp. 313–443.

Dong, Sijia et al. (2018). "A kinetic pressure effect on calcite dissolution in seawater". In: *Geochimica et Cosmochimica Acta* 238, pp. 411–423.

Gattinoni, Paola, Monica Papini, and Laura Teresa Giuseppina Scesi (2002). *Geologia Applicata. Il Rilevamento Geologico-Tecnico*. Casa Editrice Ambrosiana.

Hoegh-Guldberg, O et al. (2018). "Impacts of 1.5°C Global Warming on Natural and Human Systems". In: *Global Warming of 1.5°C. An IPCC Special Report on the impacts of global warming of 1.5°C above pre-industrial levels and related global greenhouse gas emission pathways, in the context of strengthening the global response to the threat of climate change, sustainable development, and efforts to eradicate poverty*. Intergovernmental Panel on Climate Change (IPCC), pp. 175–312.

Houpert, Loıc et al. (2015). "Seasonal cycle of the mixed layer, the seasonal thermocline and the upper-ocean heat storage rate in the Mediterranean Sea derived from observations". In: *Progress in Oceanography* 132, pp. 333–352.

Kirchner, Julia S, Andrew Berry, et al. (2020). "Reducing CO_2 Emissions of a Coal-Fired Power Plant via Accelerated Weathering of Limestone: Carbon Capture Efficiency and Environmental Safety". In: *Environmental science & technology* 54.7, pp. 4528–4535.

Kirchner, Julia S, Karsten A Lettmann, et al. (2020). "Carbon capture via accelerated weathering of limestone: Modeling local impacts on the carbonate chemistry of the southern North Sea". In: *International Journal of Greenhouse Gas Control* 92, p. 102855.

Larsen, Ole and Dieke Postma (2001). "Kinetics of reductive bulk dissolution of lepidocrocite, ferrihydrite, and goethite". In: *Geochimica et Cosmochimica Acta* 65.9, pp. 1367–1379.

Liu, Zaihua, Daoxian Yuan, and Wolfgang Dreybrodt (2005). "Comparative study of dissolution rate-determining mechanisms of limestone and dolomite". In: *Environmental Geology* 49.2, pp. 274–279.

Lyman, John and Richard H Fleming (1940). "Composition of sea water". In: *J. mar. Res* 3.2, pp. 134–146.

Masson-Delmotte, V et al. (2018). "IPCC, 2018: Summary for Policymakers." In: *Global warming of 1.5°C. An IPCC Special Report on the im-*

pacts of global warming of 1.5˚C above pre-industrial levels and related global greenhouse gas emission pathways, in the context of strengthening the global response to the threat of climate change, sustainable development, and efforts to eradicate poverty. Intergovernmental Panel on Climate Change (IPCC), p. 32.

Mitchell, Mark J et al. (2010). "A model of carbon dioxide dissolution and mineral carbonation kinetics". In: *Proceedings of the Royal Society A: Mathematical, Physical and Engineering Sciences* 466.2117, pp. 1265–1290.

Morse, John W and Shiliang He (1993). "Influences of T, S and PCO_2 on the pseudo-homogeneous precipitation of $CaCO_3$ from seawater: implications for whiting formation". In: *Marine Chemistry* 41.4, pp. 291–297.

Naviaux, John D et al. (2019). "Calcite dissolution rates in seawater: Lab vs. in-situ measurements and inhibition by organic matter". In: *Marine Chemistry* 215, p. 103684.

Page, Brad et al. (2020). *The Global Status of CCS 2020: Vital to Achieve Net Zero.*

Palandri, James L and Yousif K Kharaka (2004). *A compilation of rate parameters of water-mineral interaction kinetics for application to geochemical modeling.* Tech. rep. Geological Survey Menlo Park CA.

Parkhurst, David L, CAJ Appelo, et al. (1999). "User's guide to PHREEQC (Version 2): A computer program for speciation, batch-reaction, one-dimensional transport, and inverse geochemical calculations". In: *Water-resources investigations report* 99.4259, p. 312.

Perkins, EH et al. (1997). "Critical review of classes of geochemical computer models adaptable for prediction of acidic drainage from mine waste rock". In: *Proceedings: Fourth International Conference on Acid Rock Drainage. MEND, Ottawa, Ontario, Canada*, pp. 587–601.

Plummer, LN, TML Wigley, and DL Parkhurst (1978). "The kinetics of calcite dissolution in CO_2-water systems at 5 to 60°C and 0.0 to 1.0 atm CO_2". In: *American journal of science* 278.2, pp. 179–216.

Pokrovsky, Oleg S, Sergey V Golubev, and Jacques Schott (2005). "Dissolution kinetics of calcite, dolomite and magnesite at 25°C and 0 to 50 atm pCO_2". In: *Chemical geology* 217.3-4, pp. 239–255.

Pokrovsky, Oleg S, Sergey V Golubev, Jacques Schott, and Alain Castillo (2009). "Calcite, dolomite and magnesite dissolution kinetics in aqueous solutions at acid to circumneutral pH, 25 to 150°C and 1 to 55 atm pCO_2: New constraints on CO_2 sequestration in sedimentary basins". In: *Chemical geology* 265.1-2, pp. 20–32.

Portner, H O et al. (2019). "IPCC 2019: Summary for Policymakers". In: *In: IPCC Special Report on the Ocean and Cryosphere in a Changing Climate*. Intergovernmental Panel on Climate Change (IPCC), p. 42.

Pytkowicz, RM (1973). "Calcium carbonate retention in supersaturated seawater". In: *American Journal of Science* 273.6, pp. 515–522.

Rau, Greg H (2011). "CO_2 mitigation via capture and chemical conversion in seawater". In: *Environmental science & technology* 45.3, pp. 1088–1092.

Rau, Greg H and Ken Caldeira (1999). "Enhanced carbonate dissolution: a means of sequestering waste CO_2 as ocean bicarbonate". In: *Energy Conversion and Management* 40.17, pp. 1803–1813.

Renforth, Philip, PAE Pogge von Strandmann, and GM Henderson (2015). "The dissolution of olivine added to soil: Implications for enhanced weathering". In: *Applied Geochemistry* 61, pp. 109–118.

Righi, Davide (2020). "Analysis of enhanced pressurized weathering of limestone as a technology for CO_2 storage". Laurea magistrale. Politecnico di Milano.

Robinson, Allan and Henry Stommel (1959). "The oceanic thermocline and the associated thermohaline circulation". In: *Tellus* 11.3, pp. 295–308.

Rogelj, Joeri et al. (2018). "Mitigation pathways compatible with 1.5°C in the context of sustainable development". In: *Global Warming of 1.5°C. An IPCC Special Report on the impacts of global warming of 1.5°C above pre-industrial levels and related global greenhouse gas emission pathways, in the context of strengthening the global response to the threat of climate change, sustainable development, and efforts to eradicate poverty.* Intergovernmental Panel on Climate Change (IPCC), pp. 93–174.

Schuiling, RD and P Krijgsman (2006). "Enhanced weathering: an effective and cheap tool to sequester CO_2". In: *Climatic Change* 74.1, pp. 349–354.

Walker, James CG, PB Hays, and James F Kasting (1981). "A negative feedback mechanism for the long-term stabilization of Earth's surface temperature". In: *Journal of Geophysical Research: Oceans* 86.C10, pp. 9776–9782.

Weiner, Eugene R (2012). *Applications of environmental aquatic chemistry: a practical guide*. CRC press.